Competition for Water and Light in Closed-Canopy Forests: A Tractable Model of Carbon Allocation with Implications for Carbon Sinks

Caroline E. Farrior,* Ray Dybzinski, Simon A. Levin, and Stephen W. Pacala

Department of Ecology and Evolutionary Biology, Princeton University, Princeton, New Jersey 08544

Submitted March 22, 2012; Accepted September 29, 2012; Electronically published January 25, 2013

Online enhancement: appendixes.

abstract: The dependence of forest productivity and community composition on rainfall is the result of complex interactions at multiple scales, from the physiology of carbon gain and water loss to competition among individuals and species. In an effort to understand the role of these multiscale interactions in the dependence of forest structure on rainfall, we build a tractable model of individual plant competition for water and light. With game-theoretic analyses, we predict the dominant plant allocation strategy, forest productivity, and carbon storage. We find that the amount and timing of rainfall are critical to forest structure. Comparing two forests that differ only in the total time plants spend in water saturation, the model predicts that the wetter forest has fewer fine roots, more leaves, and more woody biomass than the drier forest. In contrast, if two forests differ only in the amount of water available during water limitation, the model predicts that the wetter forest has more fine roots than the drier forest and equivalent leaves and woody biomass. The difference in these responses to increases in water availability has significant implications for potential carbon sinks with rising atmospheric CO_2. We predict that enhanced productivity from increased leaf-level water-use efficiency during water limitation will be allocated to fine roots if plants respond competitively, producing only a small and short-lived carbon sink.

Keywords: competition, biomass allocation, water limitation, evolutionarily stable strategies, perfect-plasticity approximation.

Introduction

As the concentration of CO_2 in the atmosphere continues to rise, across many forest ecosystems, productivity is expected to increase and act as a buffer, slowing the rate of climate change through increased carbon storage (IPCC 2007; Bonan 2008). Experiments testing this prediction have shown that increased carbon storage following enhancement of CO_2 levels can be complicated by a number of factors (Norby and Zak 2011). One such complication is that enhanced productivity is often unevenly distributed among plant structures. A unit of carbon allocated to a long-lived tissue with relatively recalcitrant litter, such as woody biomass, can spend orders of magnitude longer in storage than one allocated to a short-lived tissues with relatively labile litter, such as fine roots or leaves (Luo et al. 2003). Thus, understanding changes in plant productivity alone is insufficient to accurately predict the fate of the land carbon sink. Predictive models of shifting plant allocation patterns are critical for our ability to predict whether the terrestrial biosphere has the potential to be a buffer or an accelerator of climate change.

Predicting landscape-level patterns of carbon allocation is a difficult task. Because of the complex processes and feedbacks involved in plant physiological dependence on environment and in size asymmetrical competition among individuals, simulations are often used to incorporate these mechanisms into predictions of stand-level dynamics. Forest simulators have been widely successful at predicting stand-level forest properties such as basal area and successional patterns (e.g., Horn 1975; Shugart and West 1977; Pacala et al. 1993; Moorcroft et al. 2001) and have been used to explore mechanics of competition and scaling of various plant traits (e.g., Weiner et al. 2001; Zavala and Bravo de la Parra 2005; Falster et al. 2011). However, insights gained from simulation models are constrained both by the amount of species-specific data needed to run the models and by finite parameter exploration and simulation time (Berger et al. 2008). Dybzinski et al. (2011) recently developed a mechanistically rich yet analytically tractable model of plant competition for light and nitrogen. This model successfully predicted the dominant tradeoff in allocation in forests between wood and fine roots (as opposed to one between foliage and roots) and provided new explanations for several well-established phenomena. But this model fails to explain a large portion of

* Corresponding author; e-mail: cfarrior@princeton.edu.

Am. Nat. 2013. Vol. 181, pp. 314–330.
0003-0147/2013/18103-53743$15.00.
DOI: 10.1086/669153

the variability in the data as well as some obvious patterns. These shortcomings may not be surprising, as the model applies only to water-saturated (i.e., energy- or light-limited) systems.

Water availability has long been recognized as a fundamental driver of vegetation structure (Holdridge 1967; Whittaker 1975; Walter and Breckle 1985; Woodward 1987). Yet mechanistic and predictive models of the transitions between vegetation types and variation of landscapes within them are still a challenge (Purves and Pacala 2008). Perhaps some of this difficulty arises from the stochastic nature of rainfall. Both the total amount and the distribution of rainfall in time have been shown to have significant effects on population and community structure in experimental and observational studies (Weltzin et al. 2003; Knapp et al. 2008). But these effects are mixed. For example, Fay et al. (2008) found that the effects of timing of water application can be as large as the effect of the total amount of water applied. Further, the direction of the effects of timing depends on that total amount.

Mechanistic understanding of the dependence of plant allocation strategies on water availability has become even more important in recent years (Weltzin et al. 2003). Across several CO_2 fertilization experiments, there are two common leaf-level responses: enhanced photosynthetic efficiency and increased intrinsic water-use efficiency (Ainsworth and Long 2005). Intrinsic water-use efficiency (ω) is the amount of carbon assimilated per amount of water transpired at the site of gas exchange. If one extrapolated these leaf-level responses to make predictions of productivity at the landscape level, one would predict that the proportional increase in carbon fixation in response to CO_2 fertilization should be strongest in years in which water stress is high (but not beyond the tolerance of the plants) and when plants can benefit from the increase in ω. However, in CO_2 fertilization experiments, dry years are likely to have lower responses of net primary productivity to CO_2 fertilization than wet years (Nowak et al. 2004; McCarthy et al. 2010). In addition, Peñuelas et al. (2011) found that increasing CO_2 over the past 40 years in several biomes led to significant increases in intrinsic water-use efficiency but did not lead to increased rates of biomass growth. These results contribute to uncertainty in our estimates of the potential for the terrestrial biosphere to be a buffer of climate change.

Despite the complexity of plant dependence on the timing of rainfall, remarkable success has been made in incorporating the complexities of stochastic rainfall into models of soil moisture dynamics (Rodríguez-Iturbe et al. 1999). Using this model of soil moisture dynamics, a recent simulation model made progress at predicting the dependence of plant productivity on rainfall regimes, reproducing some of the complexity observed in experiments and natural observations (Zavala and Bravo de la Parra 2005). Yet this work does not examine the potential for shifts in community composition of the water-uptake strategies by plants. Previous simple models of plant competition for water have proven to be too simple, producing paradoxical results (Gersani et al. 2001; Zea-Cabrera et al. 2006*a*, 2006*b*). In representing rainfall as a single level of constant drizzle and water as a common resource pool, these studies found that if there exists any degree of water limitation, a landscape dominated by a feasible allocation strategy is susceptible to invasions by individuals with greater investment in water uptake. Once these invasions occur, the new monoculture is full of individuals with high water uptake, which drives down availability to each individual. In these simple models, these invasions proceed until plants invest all of their productivity in water uptake and are incapable of sustaining a community. This is paradoxical, as we know that water limitation is a common phenomenon in productive plant communities.

In order to build a mechanistic understanding of the dependence of tree allocation strategies in closed-canopy forests on rainfall, we bring together basic plant physiology and a new, tractable forest-dynamics model (Purves et al. 2007; Strigul et al. 2008). We build a model that provides simple explanations for the coexistence of water limitation with productive plant communities as well as the complex results of experimental water and CO_2 additions. The model makes the two scale transitions found in mechanistic forest simulators: from the environmental resources to the individual, and from the individuals to the stand. To retain analytical tractability, we make strategic simplifications and approximations about plant allometry and physiology at the individual level. We then use the perfect-plasticity approximation (Strigul et al. 2008) to scale tractably from individual-level competition and height-structured competition for light to stand-level properties. We use game-theoretic analyses to predict the results of community dynamics. The goals of this article are to provide analytical expressions for the dependence of competitively dominant tree allocation strategies on rainfall and to derive a number of ecological insights, including a simple and realistic resolution to the tragedy of the commons for water use in plants, novel insight into the dependence of plant allocation strategies on rainfall, and an understanding of the forest carbon sink.

The Model

Here, we explain the elements of our model needed to understand the dependence of biomass allocation in closed-canopy forests on water availability. All of the elements of the model (equations and parameter definitions) can be found in table 1. For a full description of the model,

Table 1: Model elements: variables, their definitions, and key equations

Element	Units	Equation or notation	Equation number
Individual tree structure:			
Stem diameter	cm	D	
Height	m	$Z = HD^{\gamma-1}$	1
Structural biomass	kg of carbon (kg C)	$S = a_s D^{\gamma+1}$	2
Crown area	m^2	$W = a_w D^{\gamma}$	3
Constant common to allometries		$\gamma \approx 1.5$ (see app. A)	
Subscripts indicating traits of canopy and understory individuals		c and u, respectively	
Leaf area per unit crown area	$m^2\ m^{-2}$	l	
Fine-root surface area per unit crown area	$m^2\ m^{-2}$	r	
Fecundity per unit crown area	Saplings $m^{-2}\ year^{-1}$	F	
Building and respiration carbon costs of leaves and roots	kg C $m^{-2}\ year^{-1}$	c_l and c_r, respectively	
Building cost of structural biomass	kg C kg C^{-1}	$c_{b,g}$	
Carbon cost per sapling produced	kg C $sapling^{-1}$	c_f	
Water-limited plant water potential	MPa	Ψ_C	
Environmental inputs and individual resource availability:			
Light level in full sun	MJ PAR $m^{-2}\ year^{-1}$	L_0	
Proportion of time in water saturation		q	
Rain input rate during water limitation or water saturation	m $year^{-1}$	R_{dry} or R_{wet}, respectively	
Water-use efficiency	kg C m^{-1}	ω	
Conductance of water through the plant (soil to leaf)	m $MPa^{-1}\ m^{-2}\ year^{-1}$	C	
Soil-water potential at equilibrium	MPa	$\Psi_A = \min\left(\Psi_B, \frac{(R_{dry} \text{ or } R_{wet})}{\bar{r}_c C} + \Psi_C\right)$	
Light level below l leaf layers	MJ PAR	$L = L_0 e^{-kl}$	4

Individual carbon assimilation and growth rate:			
Water-saturated, leaf-level carbon assimilation	kg C m^{-2} $year^{-1}$	$a = \min(a_f L, V)$	5
Water-saturated, tree-level carbon assimilation	kg C m^{-2} $year^{-1}$	$A_L = \begin{cases} Vl & \text{if } \min(a) = V \\ \frac{V}{k}\left(1 + \ln\left(\frac{\alpha_f L_0}{V}\right) - \frac{\alpha_f L_0}{V} e^{-kl}\right) & \text{if } \min(a) = \alpha_f L \text{ and } \max(a) = V \\ \frac{\alpha_f L_0}{k}(1 - e^{-kl}) & \text{if } \max(a) = \alpha_f L \end{cases}$	6
Water limitation condition		$\Psi_A < \frac{A_L}{rC\omega} + \Psi_C$	7
Water-limited carbon assimilation	kg C m^{-2} $year^{-1}$	$A_W = rCw(\Psi_A - \Psi_C)$	8
Yearly carbon assimilation	kg C m^{-2} $year^{-1}$	$A = qA_L + (1 - q)A_W$	
Diameter growth rate	cm $year^{-1}$	$G = \frac{\alpha_w}{\alpha_s(\gamma+1)} \frac{1}{1+\zeta_{b,g}}(A - lc_l - rc_r - c_f F)$	9
Population and community dynamics:			
Mortality rate	$year^{-1}$	μ	
Subscripts indicating a trait of the invading and resident species		I and R, respectively	
Diameter of smallest canopy individual of the resident species	cm	$D_R^* = \frac{G_u}{\mu_u} \ln\left(\frac{F_c \alpha_w \Gamma(\gamma+1) G_c (R,R)^\gamma}{\mu_c^{\gamma+1}}\right)$	10
LRS of invading species (I) in the resident's (R) environment	Expected trees per lifetime	$\mathrm{LRS}(I,R) = F_c \alpha_w \Gamma(\gamma+1) \frac{G_c(I,R)^\gamma}{\mu_c^{\gamma+1}} e^{-(\mu_u/G_u)D_R^*}$	11
Evolutionarily stable/competitive strategy (ESS) satisfies these conditions		$\forall j \neq k^{ESS}$: $\mathrm{LRS}(j, k^{ESS}) < 1$ or $(\mathrm{LRS}(j, k^{ESS}) = 1$ and $\mathrm{LRS}(k^{ESS}, j) > 1)$	12

Note: Derivation of equations and their usage are presented in brief in the main text and in detail in appendix A. Values of these parameters used in graphical presentations and empirical comparisons are provided in table A1, available online (sources are provided in table A2, available online). LRS = lifetime reproductive success; PAR = photosynthetically active radiation.

including empirical justifications of functional forms used, broader discussion of extensions, and alternative usage of this model, see appendix A, available online. Also, see (Dybzinski et al. 2011) for a description of a similarly designed model with plant competition for nitrogen and light.

Individual Trees

Individual trees in the model are made out of foliage, fine roots, and structural biomass (trunk, branches, and coarse roots). As a tree grows, its basic dimensions increase. Trunk diameter (D), height of the tree (Z), total structural biomass (S), and crown area (W) are all related by allometric equations (table 1, eqq. [1]–[3]). Fine-root biomass, foliage, and fecundity of mature trees increase linearly with crown area (foliage $= lW$, fine-root surface area $= rW$, mature tree fecundity $= FW$), where mature trees are those in the canopy. We assume that understory trees do not reproduce. Each tree crown has a flat top, making l the equivalent of a leaf area index measured for an individual. Taking these building blocks together, we find that diameter growth rate (G) is approximately independent of tree size (see derivation in "Carbon Allocation and Growth" in app. A) and dependent only on resource availability per unit crown area. We allow for the possibility that leaf (l) and fine-root (r) investment strategies are responsive to changes in resource availability over a tree's lifetime.

Carbon Assimilation

We first describe scaling from the environment through physiological mechanisms to individual growth rates. Our physiological model is designed to maintain analytical tractability while incorporating, at least qualitatively, the most important mechanisms that balance water loss and carbon gain. However, the model is specifically designed to make it relatively easy to add the complexity necessary to build it into the land-surface component of a climate model (see app. A).

For this analysis, we assume that water and light are the sole limiting resources. If water availability is high enough, plants are water saturated and the rate of photosynthesis will be dependent on the capture of light by leaves. Following a simplified Farquhar photosynthesis model (Farquhar et al. 1980), leaves can perform photosynthesis at a rate proportional to their light level up to a maximum rate V (eq. [5]). This light level falls off exponentially at rate k as light travels downward through the crown of a tree, as a result of self-shading (eq. [4]). The water-saturated (energy- or light-limited) photosynthetic rate of the whole tree per unit crown area, A_L, can then be found by summing the light-dependent photosynthesis of the leaf layers of the crown (eq. [6]).

As photosynthesis occurs and plants assimilate carbon, they must open stomates to take up CO_2 from the atmosphere. As they do this, water is lost from the stomatal pore at a constant carbon-water exchange rate ω. If a plant is water limited (eq. [7]), it is not able to afford the water needed to take up the CO_2 required for the water-saturated rate of photosynthesis, A_L (A_L/ω). The maximum rate of water that plants can supply to their leaves is dependent on the total amount of fine-root surface area (rW), the conductance of water through the plant from the soil to the leaf (C), the soil-water potential (Ψ_A), and the minimum tolerable xylem water potential of the tree (Ψ_C, water supply $= WrC(\Psi_A - \Psi_C)$). This flow restricts water-limited photosynthesis, A_W, so that the demand for water does not exceed the maximum possible supply (eq. [8]).

Resource Availability

Most individual-based forest models use full spatial simulators of all trees in an area to determine the resources available to a single tree. Recent advances have determined an analytical approximation of this process. Plants are phototropic, and over time, trees in a forest bend their trunks and adjust their crowns in response to available sunlight. Making the assumption that trees are capable of foraging perfectly for light in horizontal space (the "perfect-plasticity approximation" [PPA]) is a good analytical approximation to full spatial simulators of forests where trees have tessellating crowns, especially if they have even just a small ability to bend toward light (Purves et al. 2007; Strigul et al. 2008). A model using this assumption makes accurate predictions of forest succession in the lake states region of the United States (Michigan, Wisconsin, and Minnesota; Purves et al. 2008) without spatial simulations. We take advantage of these advances and include the PPA in our model.

The assumptions behind the PPA imply that a forest canopy is filled by the crowns of the tallest individuals present and that canopy individuals shade understory individuals but not other canopy individuals. Shade cast by canopy trees is well mixed before it reaches an understory individual. It is assumed that understory individuals also efficiently partition space and do not shade one another. This creates two potential light availabilities for individuals in a forest, a canopy level and an understory level.

Soil moisture, the water available to plants, is determined by inputs from rainfall and losses from runoff, evaporation, and plant uptake. Rainfall is a stochastic process, and thus soil moisture regimes are difficult to characterize. However, the dependence of plants on these highly variable patterns can be well characterized by only

two parameters, the time in water saturation and the average soil moisture for which plants compete while water limited (C. E. Farrior, R. Dybzinski, I. Rodríguez-Iturbe, S. A. Levin, and S. W. Pacala, unpublished manuscript).

We thus use a rainfall model in this article with enough complexity to capture the effect of variability in soil moisture but enough simplicity to maintain tractability. Plants experience two different levels of rainfall as constant drizzle (there are no storms per se), R_{wet} and R_{dry}, for total proportions of the growing season q and $(1 - q)$, respectively. We assume that rainwater enters the soil at a constant drizzle and that plant uptake is effectively well mixed in the environment. That is, the water taken up by a single tree draws down the water available to all trees equally, as supported by the extensive commingling of individuals' roots in forests (Casper et al. 2003; Göttlicher et al. 2008). We further assume that soil moisture rapidly equilibrates when rainfall moves from R_{wet} to R_{dry} and vice versa.

With the assimilated carbon (A), a tree builds and maintains leaves and fine roots, increases structural biomass, and invests in reproduction. Because these expenses must equal the assimilated carbon, we can find the growth in structural biomass expressed as trunk diameter growth rate as a result of the leaf and root strategies G (eq. [9]).

At equilibrium, there are only two suites of resource levels, those experienced by canopy individuals and those experienced by understory individuals. Canopy individuals are in full sun, whereas understory individuals are shaded by the canopy layer. All trees experience the same water availability per unit area. This gives a total of two possible values of the resource-dependent properties leaf area index (l), fine-root area index (r), stem diameter growth rate (G), fecundity (F), and mortality (μ). As we are interested in allocation among leaves, fine roots, and structural biomass here, we take all species to have equivalent fecundity, canopy mortality, and understory mortality rates.

Population dynamics of the perfect-plasticity approximation (Strigul et al. 2008, with small modifications described in "Z^* Derivation" in app. A) translate these vital rates into several properties of a monoculture at equilibrium. Particularly useful expressions are the size at which trees transition from understory to canopy status (eq. [10]) and the expected lifetime reproductive success (LRS), that is, the fitness, of a target individual whose traits may differ from the monoculture at equilibrium (eq. [11]).

Analysis of the Competitively Dominant, or Evolutionarily Stable, Strategy

Adaptive-dynamics methods make the problem of predicting dominant allocation strategies straightforward (McGill and Brown 2007). To find a competitively dominant, or evolutionarily stable, strategy (ESS), if it exists, we do not need to consider every scenario of population dynamics. We consider only equilibrium monocultures and the potential for different species with differing strategies to invade from negligible population size. We use the LRS of a rare strategy as a measure of invasion success.

If LRS > 1, then on average, an individual with that strategy will be able to more than replace itself over its lifetime, making the population of the strategy grow in size and perhaps take over the community. To find the competitively dominant strategy, or ESS, we search for a strategy that cannot be invaded in this manner by any other strategy (eq. [12]; Maynard Smith and Price 1973; Maynard Smith 1982). Using pairwise invasion plots (app. C, available online; Geritz et al. 1998; fig. 1), we also determine that these solutions are convergence stable.

In this article, we restrict our predictions of ESS strategies to plant allocation to leaves, woody biomass, and fine roots. We hold all other physiological traits constant. As other leaf and wood traits are likely to vary along these water-stress and productivity gradients, potentially altering the fitness of specific allocation strategies, this analysis may be thought of as a prediction of the first-order response of allocation strategy to water availability. We leave consideration of interaction of allocation strategies with other plant traits to future work.

Results

As described above, we assume that an individual's investment in l and r may switch when it moves from the understory to the canopy. This makes l_c and r_c distinct from l_u and r_u, allowing us to treat them separately in ESS analyses. We reserve the presentation and discussion of understory strategies for appendix B, available online.

Competitive Allocation under Rainfall as a Constant Drizzle

We begin our analyses by examining the dependence of competitively dominant strategies (ESSs) of biomass allocation on rainfall levels when that rainfall comes at a single constant drizzle ($R_{wet} = R_{dry} = R$). If this drizzle is large enough, plants are always water saturated, and we find intuitive results that are equivalent to those found in several other models (e.g., Horn 1971; Givnish 1988; Tilman 1988; Dybzinski et al. 2011). If plants are water limited at all, we find the same paradoxical results as did simpler models of competition for water alone (Gersani et al. 2001; Zea-Cabrera et al. 2006*a*, 2006*b*), despite the addition of light limitation in this model. The competitive strategy is one in which a plant invests so much in fine-root biomass that it has effectively no carbon left for reproduction and growth. Yet we find that variability of rain-

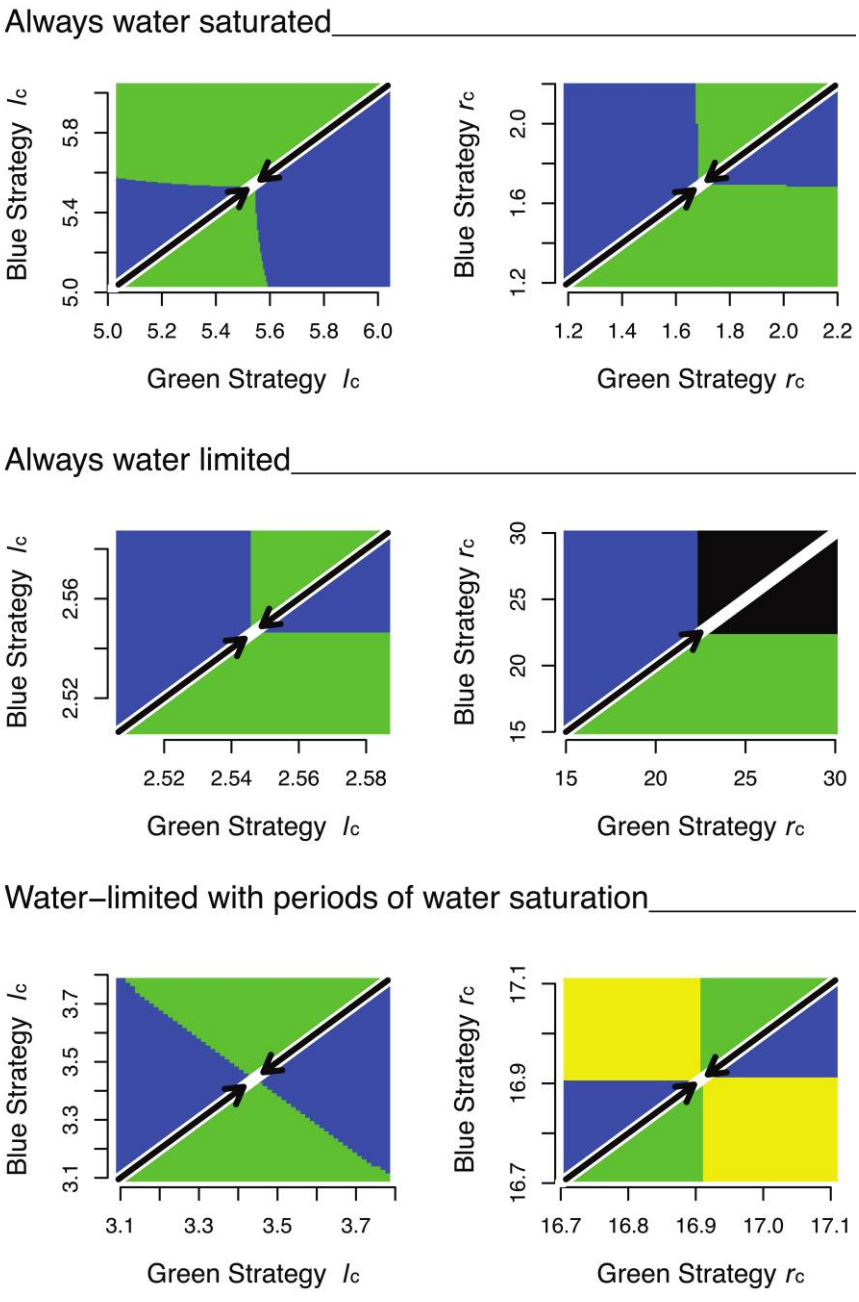

Figure 1: Pairwise invasion plots demonstrate the tragedy of the commons for water use in plants with water limitation (*middle*) and its resolution through inclusion of periods of water saturation (*bottom*). Strategies differ by leaf area index only on the left and by root area index only on the right. For each point on the graph, the outcome of an invasion of the green strategy into a monoculture of the blue strategy and vice versa are plotted with the following colors. Green indicates that the green strategy is competitively dominant in pairwise invasion tests: the green strategy can invade a monoculture of the blue strategy, but the blue strategy cannot invade a monoculture of the green strategy. Blue indicates that the blue strategy is competitively dominant. Yellow indicates that neither green nor blue is competitively dominant. Green and blue strategies can invade each other from rarity. Black indicates that neither strategy produces a closed-canopy forest in monoculture. *Top*, trees experience rainfall as constant drizzle high enough for water saturation ($R = 1.5$ m year^{-1}). *Middle*, rainfall is too low for water saturation ($R = 0.75$ m year^{-1}). *Bottom*, trees experience temporally variable rainfall, switching between high and low rainfall ($q = 0.5$, $R_{dry} = 0.75$ m year^{-1}, $R_{wet} = 1.5$ m year^{-1}). Arrows indicate the direction of movement of the resident strategy in strategy space as successful invaders become residents.

fall provides a biologically realistic and yet novel resolution to this paradox.

We first show the results for the seemingly paradoxical case without variability in rainfall. If R_{crit} is the critical level of rainfall that separates water saturation and water limitation, we find that if $R > R_{crit}$, then

$$l_{c,wet}^{ESS} = \frac{1}{k}\ln\left(\frac{\alpha_f L_0}{c_l}\right),$$
$$r_{c,wet}^{ESS} = \frac{A_L(L_0, l_c^{ESS})}{\omega C(\Psi_B - \Psi_C)}, \quad (13)$$

and if $R \leq R_{crit}$, then

$$l_{c,dry}^{ESS} = \frac{1}{k}\ln\left(\frac{\alpha_f L_0}{V(1 + \ln(\alpha_f L_0/V) - (R\omega k/V))}\right),$$
$$r_{c,dry}^{ESS} = \frac{\omega R}{c_r}, \quad (14)$$

where

$$R_{crit} = \frac{A_L(L_0, l_{c,wet}^{ESS})}{\omega}. \quad (15)$$

If rainfall is high, then the ESS strategy is equivalent to the strategy that would maximize the net carbon uptake of a forest, given unlimited water. The number of leaf layers these trees have is the number whereby the productivity of the last leaf layer is just the same as the cost to build and maintain it ($l_{c,wet}^{ESS}$). Recall that the more layers of leaves a tree has, the less productive the last layer becomes, because of self-shading. The fine-root investment these plants make is the one that supplies water at a rate that satisfies the photosynthetic demands of this number of leaves. Because R_{crit} is the water use of the ESS and $R > R_{crit}$, the soil-water potential quickly reaches the maximum (Ψ_B), and there is no competition among plants for water.

If rainfall is low, such that trees are water limited, the competitively dominant strategy, unlike the ESS under water saturation, is not the same as the strategy that would maximize the net carbon uptake of the whole forest. In this "dry" case, the soil-water potential an invader experiences depends on the fine-root investment strategy of the resident. The ESS of allocation to fine roots, expressed analytically above, is not actually feasible; plants with that strategy would spend all of their photosynthate on fine roots and have none left over for growth or fecundity. Yet there is nothing in this model that keeps the community from moving toward this unfeasible strategy (fig. 1, middle panels). If an invading strategy has a greater investment in fine roots than the resident, it is able to take up more water and do more photosynthesis than an individual of the resident strategy of equal size. This new strategy will then begin to grow in population size and eventually become the new resident. Just like the old strategy, the new strategy can be invaded by individuals with greater fine-root investment. Each of these strategies will have successively less productivity in monoculture. At equilibrium, each monoculture of these different strategies takes up the same amount of water (all of it), but the more competitive, higher–root investment strategies spend more on building and maintaining fine roots. The result is true for any degree of water limitation when rainfall is at a single constant level. That is, it does not matter how high the rainfall levels are when plants are water limited. If plants are water limited at all, there is no stable, productive allocation strategy. This result is puzzling, as we know that water limitation is a common phenomenon in plant communities with stable community composition and size structure.

Resolution to the Paradox of the Tragedy of the Commons for Water Use in Plants

We now allow for R_{wet} and R_{dry} to differ from each other. Recall that the environment may switch between R_{wet} and R_{dry} several times through the growing season. Because we assume that soil moisture equilibrates rapidly in relation to these transitions, we use only these levels and the portion of the growing seasons over which they apply (q and $1 - q$, respectively).

If R_{wet} is high enough for water saturation ($R_{wet} > R_{crit}$) and R_{dry} is low enough for water limitation (the exact condition can be found in table 2, case 3), the soil-water potential switches between its maximum and a drier water potential that depends on rainfall and plant uptake,

$$\Psi_A(R_{wet}) = \Psi_B,$$
$$\Psi_A(R_{dry}) = \frac{R_{dry}}{r_c C} + \Psi_C, \quad (16)$$

and photosynthesis (A) for the total growing season is the integration of water-saturated (A_L) and water-limited (A_W) photosynthetic rates:

$$A = qA_L(L_0, l_c) + (1 - q)A_W(R_{dry}, r_c). \quad (17)$$

The evolutionarily stable allocation strategy in this system is

$$l_c^{ESS} = \frac{1}{k}\ln\left(\frac{q\alpha_f L_0}{c_l}\right),$$
$$r_c^{ESS} = \frac{(1 - q)R_{dry}\omega}{c_r}, \quad (18)$$

Table 2: Model predictions of the evolutionarily stable strategy (ESS) allocation patterns of canopy plants

Case	Limitation during wet/dry periods	Maximum R_{dry}	l_c^{ESS}	r_c^{ESS}
1	Water saturated/water saturated	∞	$\frac{1}{k}\ln\left(\frac{\alpha_f L_0}{c_l}\right)$	$\frac{A_L(L_0, l_c^{ESS})}{C\omega(\Psi_B-\Psi_C)}$
2	Water saturated/colimited	$A_L(L_0, l_{c,\text{case 1}}^{ESS})\omega^{-1}$	$\frac{1}{k}\ln\left(\frac{\alpha_f L_0}{V(1+\ln(\alpha_f L_0/V)-(R_{dry}\omega k/V))}\right)$	$\frac{(1-q)\omega R_{dry}}{c_r}$
3	Water saturated/water limited	$A_L(L_0, l_{c,\text{case 3}}^{ESS})\omega^{-1}$	$\frac{1}{k}\ln\left(\frac{q\alpha_f L_0}{c_l}\right)$	$\frac{(1-q)\omega R_{dry}}{c_r}$
4	Colimited/water limited	$\frac{A_L(L_0, l_{c,\text{case4}}^{ESS})c_r}{\omega^2 C(1-q)R_{dry}(\Psi_B-\Psi_C)}$	$\frac{1}{k}\ln\left(\frac{q\alpha_f L_0}{c_l}\right)$	$\frac{A_L(L_0, l_c^{ESS})}{C\omega(\Psi_B-\Psi_C)}$

Note: Analytical formulas are separated by cases that are ordered by decreasing R_{dry}. The maximum R_{dry} for the case is given. The minimum is equal to the maximum of the next case. Cases are associated with particular limitation conditions during wet (R_{wet} for q) and dry (R_{dry} for $(1-q)$) periods. By "colimitation" we mean plants that are at the point just between water saturation and water limitation. The strategies presented here are the leaf area index and root area index of ESS plants. The third axis of plant allocation, growth of woody biomass, is not presented but may be easily calculated using equation (9). All of these results are illustrated for default parameter values in figure 2.

and the photosynthate available for fecundity and growth of the competitively dominant plant strategy in monoculture when it is in the canopy is now

$$A - c_l l_c - c_r r_c = q\frac{V}{k}\left(1 + \ln\left(\frac{\alpha_f L_0}{V}\right) - \frac{c_l}{qV}\right) - \frac{c_l}{k}\ln\left(\frac{q\alpha_f L_0}{c_l}\right). \quad (19)$$

Using parameter values given in table A1, available online, we find that this is positive for $q > 0.3$. That is, there exists a feasible competitively dominant tree strategy if water limitation occurs for less than 70% of the growing season. The existence of water saturation moderates the proliferation of roots and produces a competitively dominant strategy with a stable positive monoculture abundance. In environments that are chronically water limited (more than 70% of the growing season), the model still predicts an unfeasible ESS for forests. We suggest that in such areas, other forms of vegetation will be competitively dominant.

Effects of Rainfall on Evolutionarily Stable Tree Allocation Strategies in Closed-Canopy Forests

The above ESS is not general because it assumes that the wet season is water saturated and that water is the sole limiting resource in the dry season. We now look at the full range of R_{wet}, R_{dry}, and q. The dependence of the ESS on R_{wet} is simple. If R_{wet} is below R_{crit}, then a closed-canopy forest is not stable, for the same reasons that cause the paradoxical tragedy-of-the-commons results above. If R_{wet} is above this value, then the dominant strategy does not depend on R_{wet}. The dependence of the dominant allocation strategy on R_{dry} and q is more complicated. There are four separate analytical cases of ESS allocation patterns. We explain these here. All results in this section apply when R_{wet} is above the critical value and thus high enough to satisfy the demand of the leaves. Mathematical definitions and expressions of the results in each of the four cases are presented in table 2 and illustrated in figure 2. Pairwise invasion plots for one numerical example of each case are provided in appendix C.

The four analytical cases are numbered in order of decreasing R_{dry}. We suspect that cases 1 and 4 are outside realistic parameter space. When R_{dry} is very high (case 1) or very low (case 4), the competitively dominant strategy results in maximum soil-water potential and competition among roots has no effect on plants, but for very different reasons. In case 1, R_{dry} is high enough that plants are water saturated all year; thus, the conditions and ESSs of l_c and r_c are identical to $l_{c,wet}^{ESS}$ and $r_{c,wet}^{ESS}$, described above. In case 4, R_{dry} is so low and the time in water limitation is so low (q is high) that the total productivity of water-limited days is low. It is so low, in fact, that the roots needed for competitive uptake (described below) take up water slower than the rate of water input during water limitation, R_{dry}. Thus, soil-water potential goes to the maximum, and there is no competition for water among roots.

The bulk of feasible parameter space falls into cases 2 and 3. Conditions for these cases are perhaps more relevant to the majority of closed-canopy forests across the globe than conditions for cases 1 and 4. Here, R_{dry} takes on intermediate values. Soil-water potential is low enough to be water limiting during dry periods ($1-q$ with R_{dry}) and high enough to be water saturated in wet periods (q with R_{wet}). In these cases, the dominant allocation strategies are influenced strongly by root competition.

As R_{dry} decreases and we move out of case 1 (plants completely water saturated) to case 2 (colimitation of light and water during dry periods), the ESS begins to lose leaf layers. The point of transition from case 1 to case 2 is the

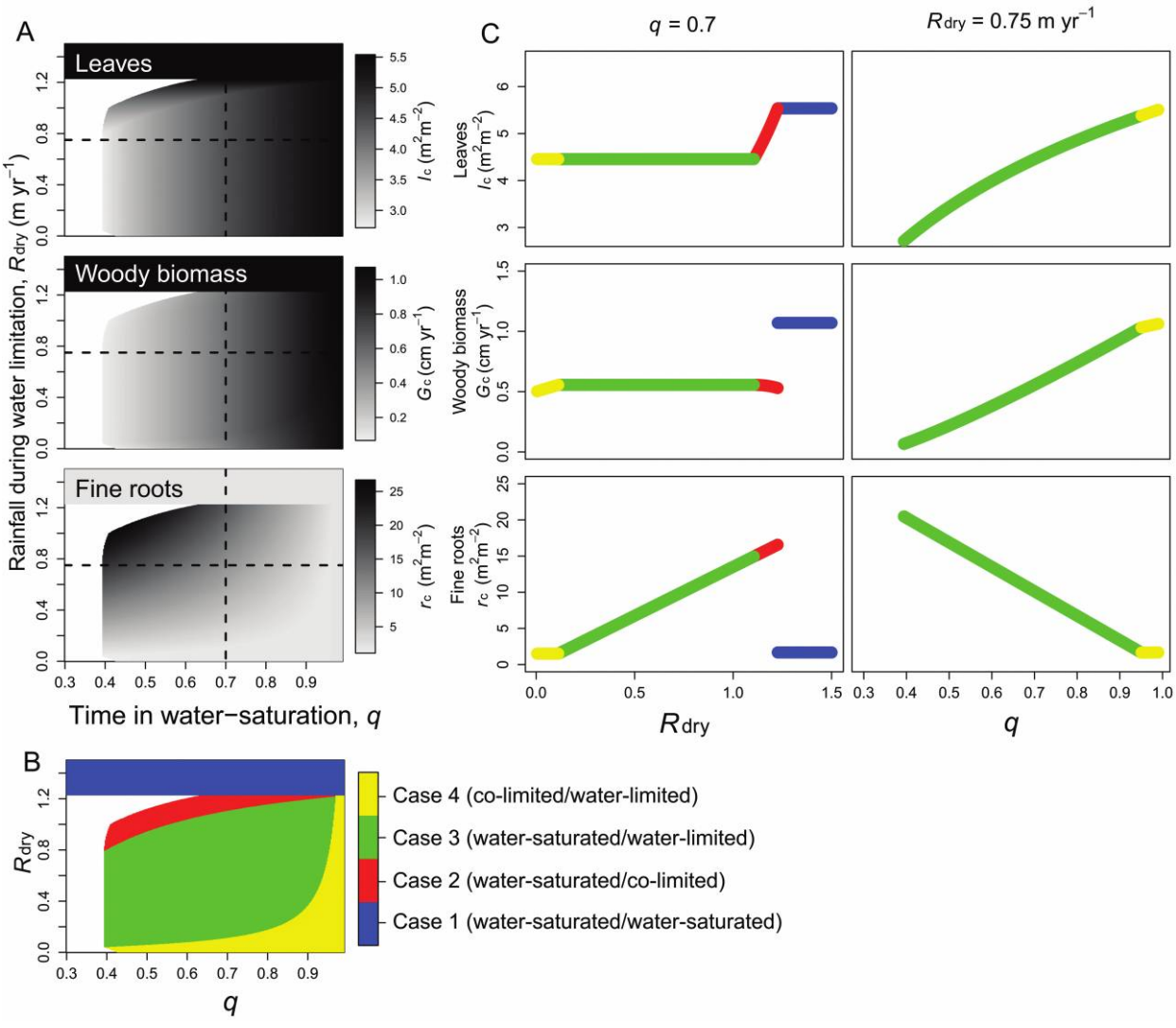

Figure 2: Biomass allocation and productivity of competitive plants depend on timing of rainfall. The competitively dominant, or environmentally stable, strategy (ESS) is described by l_c, leaf area index (top panels in *A* and *C*); G_c, the stem-diameter growth rate (middle panels in *A* and *C*); and r_c, the fine-root area index (bottom panels in *A* and *C*). *A*, Dependence of competitively dominant strategies on rainfall: q is the total portion of the growing season in water saturation, and R_{dry} is the rate of constant rainfall input during water limitation. White space indicates that the combination of rainfall parameters does not support a stable, closed-canopy forest. *B*, Dependence of plant limitation and analytical formulas for ESSs (table 2) on q and R_{dry}. *C*, Cross sections (along dashed lines in *A*) illustrate the dependence of ESSs on rainfall parameters separately ($q = 0.7$ and $R_{dry} = 0.75$).

first point where the water supply rate is less than the maximum light-limited demand. Now leaves are not being used to their maximum potential during dry periods, and it pays the plant to drop some of its most shaded and least productive leaves. This ESS drops just the right number of leaves to maintain colimitation during dry periods (fig. 2*B*; table 2; case 2 l_c^{ESS}). Within this case, the fine root : foliage ratio of the ESS increases as rainfall decreases, yet r_c^{ESS} decreases, for reasons that are described below.

As R_{dry} continues to decrease and we move from case 2 (colimitation during dry periods) to case 3 (water limitation during dry periods), the ESS stops shedding leaf layers. Here, the most shaded leaf is productive enough during the wet periods to pay for its costs during the dry periods. The value of R_{dry} at which trees shift to this strategy increases with q, or the length of time they can profit from their most shaded leaves (table 2, case 3, maximum R_{dry}). Despite the independence of l_c^{ESS} from R_{dry}, r_c^{ESS} continues to decrease with decreasing R_{dry}. We find that the ESS fine root : foliage ratio is proportional to R_{dry} and time

in water limitation $(1 - q)$, a result unique to this model:

$$r^{\mathrm{ESS}}_{\mathrm{c,case2,case3}} = \frac{(1 - q)\omega R_{\mathrm{dry}}}{c_{\mathrm{r}}}. \quad (20)$$

In both case 2 and case 3, trees experience water limitation. That is, there is a portion of the growing season when a plant's carbon gain is proportional to the amount of water it takes up. If a plant has more roots than the rest of the plants in a community, it will be able to take up more than its share of water. If the carbon gained from this strategy $((1 - q)\omega R_{\mathrm{dry}} r_{\mathrm{c,invader}}/r_{\mathrm{c,resident}})$ is greater than the respiration and maintenance costs of the extra roots $(c_{\mathrm{r}} r_{\mathrm{c,\,invader}})$, then the invader will be more productive than the resident and will grow in population size. Once this invader takes over the community and becomes the resident, the benefit of the extra roots is negated, because the equilibrium water potential decreases while the costs of the extra roots remain. This results in a new resident that is actually less productive in monoculture than the resident it replaced. Replacements like this will proceed until the benefits of added roots during invasion do not outweigh the associated construction and maintenance costs. The evolutionarily stable root strategy increases with R_{dry} because the benefits during invasion depend positively on R_{dry}. Thus, higher R_{dry} requires a higher r_{c} to be the competitive dominant. Higher q, on the other hand, decreases the amount of time plants spend in competition for water, decreasing the ESS r_{c}.

This ESS is the result of a tragedy of the commons. Trees invest in roots that cancel the value of the dry days. It is easily shown that net carbon assimilation of all dry days equals the fine-root costs for the year. This competitive investment can go as far as making closed-canopy forests unstable. Low q levels and high levels of R_{dry} drive the overinvestment in roots to make closed-canopy forests impossible in monoculture (see nonviable strategies between cases 1 and 2 in fig. 2*A*).

Predictions for ESS values of G_{c} can be seen in figure 2. Growth rates increase with the total time in water saturation (q) and are mostly independent of the rainfall level of dry periods (R_{dry}), despite the large changes in root investment with R_{dry}. As described above, the benefits of the extra roots on the dry days exactly cancels their costs, resulting in no influence on the growth rate.

Model Comparison with Natural Forests

Empirical tests of the predicted relationship between tree structure and rainfall are complicated by the idealized rainfall in the model. For example, what are the values of R_{dry} and q in any location? Here, we offer a qualitative analysis that compares the range of allocation strategies predicted by the model with those in a data set of closed-canopy forests from across the globe. The data come from a synthesis of Fluxnet data by Luyssaert et al. (2007).

Figure 3 shows the breadth of model predictions for all rainfall regimes that create stable closed-canopy forests. These predictions were made with the values reported in table A1, some of which are specific to temperate deciduous forests, making the model more likely to match data from such forests (black circles). Case 3, where competitively dominant trees are solely water limited on dry days and water saturated on wet days, is responsible for the majority of the spread in these points; thus, explanations of these patterns rely primarily on the analytical results of case 3.

Our model predicts, and the data show, a strong trade-off between allocation of net primary productivity (NPP) to structural biomass and that to fine roots but a weak relationship between allocation of NPP to foliage and that to fine roots and between allocation of NPP to structural biomass and that to foliage. Shifts in rainfall regimes in both q and R_{dry} explain the dominant trade-off between stem wood and fine roots. As q increases and plants become more productive, competitively dominant strategies should invest more in structural biomass and invest less in fine roots. With greater R_{dry}, dominant trees should have higher investment in fine roots because of greater competition for that water (as discussed above) and should have proportionally less investment in structural biomass as a result of the large root cost.

Figure 3*B* compares the breadth of potential model predictions for patterns of yearly productivity of foliage, structural biomass, and fine roots against total productivity with the forest data from across the globe. Here, longer periods of water saturation (high q) are expected to result in sites with higher total NPP, foliage NPP, and structural-biomass NPP but lower fine-root NPP, because of release from water limitation. Higher rainfall on water-limited days (high R_{dry}) is also expected to result in higher total NPP, but foliage NPP is largely unresponsive, and fine-root NPP is expected to increase as a result of increased competitive pressure.

The Dependence of Carbon Sinks on Allocation Strategy

Shifts in allocation from short- to long-lived tissues and vice versa have significant effects on carbon storage in the live biomass (kg C m^{-2}) of an ecosystem. Because we have not included a full physiological model tying atmospheric carbon concentration to leaf-level carbon gain and water loss, we cannot predict the quantitative effect of an increased concentration of CO_2 in the atmosphere. However, we can make some qualitative predictions. A one-time

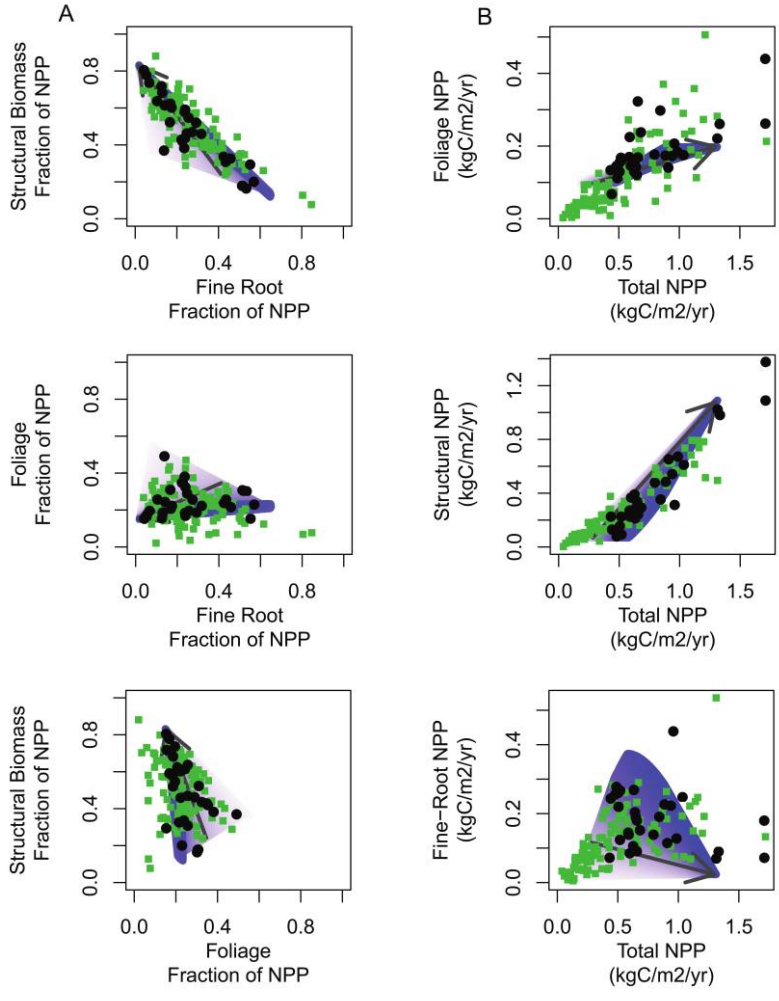

Figure 3: Comparison of model predictions of forest allocation patterns with forests from across the globe. Model predictions are shaded in blue and were made by exhausting the range of rainfall parameters that produce stable, closed-canopy forests. The intensity of the blue increases with rainfall during dry days, R_{dry}. Arrows follow increasing time in water saturation, q, of model predictions. Black circles and green squares represent data from separate closed-canopy forest Fluxnet sites (Luyssaert et al. 2007). Black circles distinguish temperate deciduous forests, which the model predictions are specifically parameterized for, from all other forest types represented in the data. *A*, Trade-offs among relative allocation of net primary productivity (NPP) to fine roots, foliage, and structural biomass. *B*, Relationship between total NPP and NPP in foliage, structural biomass, and fine roots.

permanent increase in the atmospheric concentration of CO_2 will have two main direct effects in our model. It will directly increase the maximum rate of photosynthesis of a leaf (V) because of increased carboxylation efficiency and decreased photorespiration.

It will also increase intrinsic water-use efficiency (ω) as higher atmospheric CO_2 increases the rate of diffusion of CO_2 relative to that of water on the surface of a leaf. We focus our analysis exclusively on case 3, where plants move from strict water limitation to strict water saturation as R switches from R_{dry} to R_{wet}, because this case covers most locations in our comparison with natural forests (fig. 3).

We find that whether plants respond to the changes in V and ω by adjusting their allocation patterns to match the new evolutionarily stable allocation strategy can have a significant influence on the size and longevity of a temporary carbon sink (fig. 4). To demonstrate this, we present two scenarios of plant responses to increases in ω and V: (1) plants do not change the amount of biomass they allocate to leaves (l_c) and fine roots (r_c) in response to the increase in atmospheric CO_2 (fig. 4, solid line), and (2) plant communities alter their l_c and r_c to reflect the changes in competitive allocation strategy that follow the perturbation of the environment (fig. 4, dashed line).

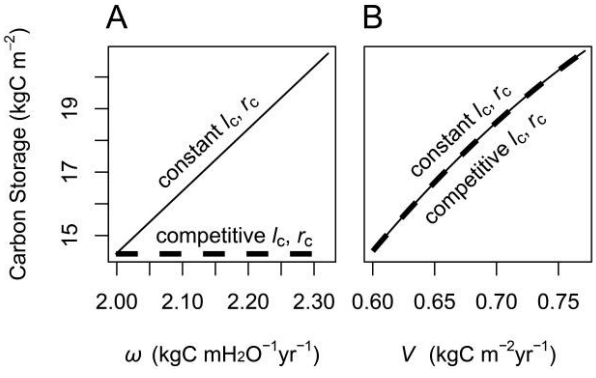

Figure 4: Carbon storage for plants with constant (solid line) and competitive (dashed line) investment in leaf and fine-root area indexes under increasing values of CO_2-correlated environmental parameters: water-use efficiency ω (*A*) and maximum photosynthetic rate V (*B*). Default values used in the rest of the article are the lowest values of ω and V. Constant leaf and root area indexes (solid line) were constrained to the competitive l_c and r_c, respectively, under these default conditions.

Steady state carbon storage in live biomass of a monoculture in our model is the sum of carbon stored in woody biomass, leaves, and fine roots:

$$\text{carbon storage} \approx \frac{\alpha_s(\gamma + 1)}{\alpha_w}\frac{G_c}{\mu_c} + l_c\text{LMA} + r_c\text{RMA}. \quad (21)$$

LMA and RMA are the leaf mass per unit area and fine-root mass per unit area, respectively (kg C m^{-2}). When plants hold l_c and r_c constant, changing ω influences only the carbon stored in woody biomass:

$$\left.\frac{\partial \text{carbon storage}}{\partial \omega}\right|_{l_c, r_c \text{ constant}} = \frac{(1-q)R_{dry}}{1 + c_{b,g}}\frac{1}{\mu_c}, \quad (22)$$

producing a large and long-lived carbon sink. Whereas if plants shift their l_c and r_c to the competitively dominant strategy, the increase in carbon storage comes from fine roots alone:

$$\left.\frac{\partial \text{carbon storage}}{\partial \omega}\right|_{l_c, r_c \text{ competitive}} = \frac{(1-q)R_{dry}}{c_r}\text{RMA}, \quad (23)$$

producing a small and short-lived carbon sink.

Changes in carbon storage due to an increase in V, however, do not depend on whether the plants track the new ESS. The ESS l_c and r_c do not depend on V in case 3, where plants are light limited and the productivity of the least productive leaf does not depend on the maximum photosynthetic rate, V:

$$\left.\frac{\partial \text{carbon storage}}{\partial V}\right|_{l_c, r_c \text{ constant or competitive}} = \frac{(q/k)\ln(\alpha_l L_0/V)}{1 + c_{b,g}}\frac{1}{\mu_c}. \quad (24)$$

Thus, if enhanced atmospheric CO_2 increases maximum photosynthetic rates, whether plants track a competitive ESS or not, we predict a large, long-lived carbon sink whose longevity scales as the longevity of canopy trees (μ_c^{-1}, i.e., a century).

Discussion

Depending on Timing, Changes in Rainfall Can Have Directly Opposite Effects on Tree Allocation Strategies

We have found that the relationship between competitively dominant tree allocation strategies and rainfall depends critically on the timing of that rainfall. If additional rainfall comes at a time when trees are already water saturated, then it has no effect. If additional rainfall has the effect of turning water-limited periods into water-saturated periods, then the competitive strategy shifts in a way that follows conventional predictions. Competitive trees invest less in fine roots and more in foliage and grow faster because of the decrease in belowground scarcity. If the additional rainfall comes during a period of water limitation, then increasing the water availability (but not enough to alleviate water limitation all together) shifts the ESS in an unexpected direction. The competitive trees invest more in fine roots, with no change in foliage or growth rate.

Resolving the Paradox of the Tragedy of the Commons for Water Use

The result that competition for water results in a tragedy of the commons is demonstrated most clearly in the case of constant rainfall through the growing season. In this case, any water limitation at all favors invasions by trees with ever greater investment in fine roots and ever less carbon allocated to growth and reproduction, making stable closed-canopy forests impossible.

Similar paradoxical results have been found before in other simple models of plant competition for water (Gersani et al. 2001; Zea-Cabrera et al. 2006*a*, 2006*b*). We have found, however, that the variable nature of soil moisture and evaporative demand obviates the paradox of the tragedy of the commons for water use as Zea-Cabrera et al. (2006*a*, 2006*b*) described it. Periods of water saturation restrain fine-root investment to realistic levels, permitting

the formation of closed-canopy forests. Although no longer paradoxical, a competitive investment in roots by dominant plants persists in this model. Unless plants are always water saturated, we predict that competitively dominant plants have an investment in roots that makes them less productive in terms of growth and fecundity than they would be if they evolved without the threat of invasion by other strategies.

An alternative resolution to the paradox of the tragedy of the commons for water use is that in competition for water, root systems become territorial and thus segregate water belowground (van Wijk and Bouten 2001; Zea-Cabrera et al. 2006*a*, 2006*b*). If root systems of plants were sufficiently segregated and horizontal mobility of soil water were sufficiently low, then a plant would invest in the roots needed to take up that water at an optimal rate without a neighbor stealing it and thus would not be confronted with the tragedy of the commons. This might occur in shrub steppe and desert communities where plant density is low. In closed-canopy forests, however, root systems overlap extensively (Casper et al. 2003; Göttlicher et al. 2008). For example, excavations of 18 root systems in New York revealed an average root : crown area ratio of 4.5 (Stout 1956), and soil cores in Panama contain roots of 4.67 species, on average (Jones et al. 2011). Thus, spatial segregation of roots is unlikely to provide the correct explanation of the resolution of the tragedy of the water-use commons in closed-canopy forests. In contrast, the resolution of the paradox offered in this article—fluctuating water availability—is present in nearly all plant communities.

Unlike root systems, the crowns of canopy trees in both our model and nature appear to be territorial because they overlap little (Jacobs 1955; Putz et al. 1984), a phenomenon known as crown shyness. Because of crown shyness, an individual canopy tree can manage its own self-shading. This allows the tree to avoid a tragedy of the light-use commons and to invest in leaves that optimize both individual- and community-level productivity.

Model Comparison with Data

We found that the model predicts patterns of allocation among foliage, fine roots, and structural biomass in forests from across the globe (fig. 3*A*). The strongest trade-off in the data and in model predictions was between structural biomass and fine roots. This can be explained by the shifting importance of competition for light (high q, high allocation to woody biomass) and competition for water (low q, high allocation to fine roots), whereas variability in these patterns is explained by the shifting of allocation to fine roots with no change in allocation to woody biomass (changing R_{dry}). We did not predict, nor did the data show, significant trade-offs between foliage and fine roots or between foliage and structural biomass.

The breadth of model predictions also captured the observed variability in relationships between total NPP and the NPP of structural biomass and fine roots but not that for foliage (fig. 3*B*). The inability of our model to capture the variability in foliage NPP, given total NPP, is likely because of variation in physiological traits of trees that are correlated with differences in total productivity. High-productivity sites are likely to be dominated by trees that are more shade tolerant than trees in low-productivity sites. This often means lower values of V for leaves and thus lower respiration rates (lower c_l), making higher foliage values possible.

Using similar techniques for predicting dominant tree strategies, a model of mechanistic competition for light and nitrogen by Dybzinski et al. (2011) also compared model predictions with the data in figure 3. Although we assume that trees have unlimited nitrogen and compete for water and light, Dybzinski et al. assumed that trees have unlimited water and compete for nitrogen and light. The predictions from Dybzinski et al. match the data as well as ours do, except in one respect. Dybzinski et al. predict a negative relationship between fine-root NPP and total NPP, whereas our model predicts a positive relationship at low NPP that transitions to a flat relationship, as is seen in the data.

For water-limited trees, increasing total NPP across a landscape is driven by both increasing time in water saturation (q) and water availability while the trees are water limited (R_{dry}). For the most common case, case 3, increases in q and R_{dry} have opposing effects on fine-root investment, explaining the variability in the data (fig. 3). At low values of NPP, plants are in case 2, where their roots supply just enough water to meet their demand on dry days. This makes plants effectively water saturated for the whole year, and their NPP no longer responds to q but only to R_{dry}. So increases in NPP at low NPP occur because of changes in R_{dry} alone and reveal positive effects on fine roots without the confounding effects of q.

Competitive Allocation Can Significantly Shift Trajectories of Carbon Storage

One of the largest sources of uncertainty in climate models is the size of the carbon sink in the biosphere (Friedlingstein et al. 2006). Although it has long been established that the individual leaves respond to added CO_2 by increasing photosynthesis and decreasing stomatal conductance, experimental CO_2 fertilization has not resolved the question of whether this translates into an increase in ecosystem carbon storage (Norby and Zak 2011). Some experimental additions have led to initial increases in woody

biomass growth, but this response has diminished over time in several experiments (Körner et al. 2005; Norby et al. 2010). Determining mechanisms of downregulation, the disconnect between leaf-level and ecosystem responses to CO_2, is critical to our understanding of carbon storage in forests.

Our model predicts a novel mechanism of downregulation in forest carbon sinks. If instantaneous water-use efficiency increases, then plants will immediately become more productive and grow faster, storing more carbon. After these plants have had a chance to adjust their standing biomass of foliage and fine roots, however, they will, if they are competitive (i.e., if they track the ESS), shift all of the increase in productivity to fine roots, turning the carbon sink into a temporary carbon source until the net effect of fertilization has almost disappeared. The timescale over which this sink becomes a source could be as short as a single year if individuals have the plasticity to track the shifting conditions. However, if replacement of individuals or species is required to shift to the new ESS, then the downregulation of the carbon sink may occur only after decades or centuries. This prediction has important consequences for the testing of predictions about the future of the carbon sink. A decade-long experiment may not be long enough to observe the change in competitive allocation strategies that would occur. This mechanism of downregulation through shifts in competitive allocation patterns could explain why significant increases in water-use efficiency in forests across the globe have not led to significant carbon sinks (Peñuelas et al. 2011), why carbon fertilization responses are not strongest during drier years (Nowak et al. 2004), and why experiments have seen responses to fertilization diminish over time (Körner et al. 2005; Norby et al. 2010). Alternatively, competitive allocation responses to increases in photosynthetic efficiency do not result in a downregulation of carbon sinks. Carbon sinks derived from this increase in productivity should be large and long-lived.

We have considered direct effects of CO_2 fertilization in our model, but there may also be indirect effects. Increased instantaneous water-use efficiency should not only increase plant-level carbon assimilation during water limitation but also increase the time plants spend in water saturation. The condition for water saturation ($R > R_{crit}$) is more likely to be met with higher ω. Because real soil moisture dynamics actually follow smooth transitions between water limitation and water saturation, it follows that lowering the water-saturation threshold will increase the proportion of time spent in water saturation, q. Just as R_{dry} and q had opposing effects on fine-root biomass, described above, ω and q have opposing effects on carbon storage. When q increases, productivity increases and ESS allocation to fine roots decreases, favoring increased foliage and growth of woody biomass. For nitrogen-saturated forests, unlike increases in ω, holding the investment in fine-root biomass constant under increases in water saturation significantly underestimates the size of a potential carbon sink. The net result of competitive allocation shifts due to increased ω and q on carbon storage depends on the specific rainfall regime of a forest. Thus, accurate predictions of shifts in carbon storage in a specific site will require a model of realistic rainfall with continuous soil moisture probabilities.

Acknowledgments

We thank S. Batterman, L. Hedin, H. Horn, S. Keel, J. Lichstein, E. Shevliakova, D. Tilman, and A. Wolf for helpful discussions and D. Menge and two anonymous reviewers for helpful comments on the manuscript. We thank all site investigators, their funding agencies, the various regional flux networks (Afriflux, AmeriFlux, AsiaFlux, CarboAfrica, CarboEurope-IP [integrated project], ChinaFlux, Fluxnet-Canada, KoFlux, LBA [Large-Scale Biosphere-Atmosphere Experiment in Amazonia], NECC [Nordic Centre for Studies of Ecosystem Carbon Exchange], OzFlux, TCOS [Terrestrial Carbon Observation System]-Siberia, USCCC [United States–China Carbon Consortium]), and the Fluxnet project, whose support is essential for obtaining the measurements without which the type of integrated analyses conducted in this study would not be possible. We gratefully acknowledge the support of the National Science Foundation Graduate Research Fellowship (DGE-0646086), the Defense Advanced Research Projects Agency (DARPA; HR0011-09-1-055), the Carbon Mitigation Initiative (CMI), and the USDA Forest Service.

Literature Cited

Ainsworth, E. A., and S. P. Long. 2005. What have we learned from 15 years of free-air CO_2 enrichment (FACE)? a meta-analytic review of the responses of photosynthesis, canopy properties and plant production to rising CO_2. New Phytologist 165:351–372.

Berger, U., C. Piou, K. Schiffers, and V. Grimm. 2008. Competition among plants: concepts, individual-based modelling approaches, and a proposal for a future research strategy. Perspectives in Plant Ecology, Evolution, and Systematics 9:121–135.

Bonan, G. B. 2008. Forests and climate change: forcings, feedbacks, and the climate benefits of forests. Science 320:1444–1449.

Casper, B. B., H. J. Schenk, and R. B. Jackson. 2003. Defining a plant's belowground zone of influence. Ecology 84:2313–2321.

Dybzinski, R., C. Farrior, A. Wolf, P. B. Reich, and S. W. Pacala. 2011. Evolutionarily stable strategy carbon allocation to foliage, wood, and fine roots in trees competing for light and nitrogen:

an analytically tractable, individual-based model and quantitative comparisons to data. American Naturalist 177:153–166.

Falster, D. S., A. Brännström, U. Dieckmann, and M. Westoby. 2011. Influence of four major plant traits on average height, leaf-area cover, net primary productivity, and biomass density in single-species forests: a theoretical investigation. Journal of Ecology 99: 148–164.

Farquhar, G. D., S. von Caemmerer, and J. A. Berry. 1980. A biochemical model of photosynthetic CO_2 assimilation in leaves of C_3 species. Planta 149:78–90.

Fay, P. A., D. M. Kaufman, J. B. Nippert, J. D. Carlisle, and C. W. Harper. 2008. Changes in grassland ecosystem function due to extreme rainfall events: implications for responses to climate change. Global Change Biology 14:1600–1608.

Friedlingstein, P., P. Cox, R. Betts, L. Bopp, W. von Bloh, V. Brovkin, P. Cadule, et al. 2006. Climate-carbon cycle feedback analysis: results from the C^4MIP model intercomparison. Journal of Climate 19:3337–3353.

Geritz, S. A. H., É. Kisdi, G. Meszéna, and J. A. J. Metz. 1998. Evolutionarily singular strategies and the adaptive growth and branching of the evolutionary tree. Evolutionary Ecology 12:35–57.

Gersani, M., J. S. Brown, E. E. O'Brien, G. M. Maina, and Z. Abramsky. 2001. Tragedy of the commons as a result of root competition. Journal of Ecology 89:660–669.

Givnish, T. J. 1988. Adaptation to sun and shade: a whole-plant perspective. Australian Journal of Plant Physiology 15:63–92.

Göttlicher, S., A. Taylor, H. Grip, N. Betson, E. Valinger, M. Högberg, and P. Högberg. 2008. The lateral spread of tree root systems in boreal forests: estimates based on ^{15}N uptake and distribution of sporocarps of ectomycorrhizal fungi. Forest Ecology and Management 255:75–81.

Holdridge, L. R. 1967. Life zone ecology. Tropical Science Center San José, Costa Rica.

Horn, H. S. 1971. The adaptive geometry of trees. Princeton University Press, Princeton, NJ.

———. 1975. Forest succession. Scientific American 232:90–98.

IPCC (Intergovernmental Panel on Climate Change). 2007. Climate change 2007: synthesis report. Contribution of Working Groups I, II, and III to the Fourth Assessment of the Intergovernmental Panel on Climate Change. IPCC, Geneva, Switzerland.

Jacobs, M. R. 1955. Growth habits of the eucalypts. Commonwealth Forestry and Timber Bureau, Commonwealth of Australia, Canberra.

Jones, F. A., D. L. Erickson, M. A. Bernal, E. Bermingham, W. J. Kress, E. A. Herre, H. C. Muller-Landau, and B. L. Turner. 2011. The roots of diversity: below ground species richness and rooting distributions in a tropical forest revealed by DNA barcodes and inverse modeling. PloS ONE 6:e24506.

Knapp, A. K., C. Beier, D. D. Briske, A. T. Classen, Y. Luo, M. Reichstein, M. D. Smith, et al. 2008. Consequences of more extreme precipitation regimes for terrestrial ecosystems. BioScience 58:811–821.

Körner, C., R. Asshoff, O. Bignucolo, S. Hättenschwiler, S. G. Keel, S. Peláez-Riedl, S. Pepin, R. T. W. Siegwolf, and G. Zotz. 2005. Carbon flux and growth in mature deciduous forest trees exposed to elevated CO_2. Science 309:1360–1362.

Luo, Y., L. W. White, J. G. Canadell, E. H. DeLucia, D. S. Ellsworth, A. Finzi, J. Lichter, and W. H. Schlesinger. 2003. Sustainability of terrestrial carbon sequestration: a case study in Duke Forest with inversion approach. Global Biogeochemical Cycles 17:1021.

Luyssaert, S., I. Inglima, M. Jung, A. D. Richardson, M. Reichstein, D. Papale, S. L. Piao, et al. 2007. CO_2 balance of boreal, temperate, and tropical forests derived from a global database. Global Change Biology 13:2509–2537.

Maynard Smith, J. 1982. Evolution and the theory of games. Cambridge University Press, Cambridge.

Maynard Smith, J., and G. R. Price. 1973. The logic of animal conflict. Nature 246:15–18.

McCarthy, H. R., R. Oren, K. H. Johnsen, A. Gallet-Budynek, S. G. Pritchard, C. W. Cook, S. L. Ladeau, R. B. Jackson, and A. C. Finzi. 2010. Re-assessment of plant carbon dynamics at the Duke free-air CO_2 enrichment site: interactions of atmospheric $[CO_2]$ with nitrogen and water availability over stand development. New Phytologist 185:514–528.

McGill, B. J., and J. S. Brown. 2007. Evolutionary game theory and adaptive dynamics of continuous traits. Annual Review of Ecology, Evolution, and Systematics 38:403–435.

Moorcroft, P. R., G. C. Hurtt, and S. W. Pacala. 2001. A method for scaling vegetation dynamics: the ecosystem demography model (ED). Ecological Monographs 71:557–586.

Norby, R. J., J. M. Warren, C. M. Iversen, B. E. Medlyn, and R. E. McMurtrie. 2010. CO_2 enhancement of forest productivity constrained by limited nitrogen availability. Proceedings of the National Academy of Sciences of the USA 107:19368–19373.

Norby, R. J., and D. R. Zak. 2011. Ecological lessons from free-air CO_2 enrichment (FACE) experiments. Annual Review of Ecology, Evolution, and Systematics 42:181–203.

Nowak, R. S., D. S. Ellsworth, and S. D. Smith. 2004. Functional responses of plants to elevated atmospheric CO_2: do photosynthetic and productivity data from FACE experiments support early predictions? New Phytologist 162:253–280.

Pacala, S. W., C. D. Canham, and J. A. Silander Jr. 1993. Forest models defined by field measurements. I. The design of a northeastern forest simulator. Canadian Journal of Forest Research 23: 1980–1988.

Peñuelas, J., J. G. Canadell, and R. Ogaya. 2011. Increased water-use efficiency during the 20th century did not translate into enhanced tree growth. Global Ecology and Biogeography 20:597–608.

Purves, D. W., J. W. Lichstein, and S. W. Pacala. 2007. Crown plasticity and competition for canopy space: a new spatially implicit model parameterized for 250 North American tree species. PloS ONE 9:e870.

Purves, D. W., J. W. Lichstein, N. Strigul, and S. W. Pacala. 2008. Predicting and understanding forest dynamics using a simple tractable model. Proceedings of the National Academy of Sciences of the USA 105:17018–17022.

Purves, D., and S. Pacala. 2008. Predictive models of forest dynamics. Science 320:1452–1453.

Putz, F. E., G. G. Parker, and R. M. Archibald. 1984. Mechanical abrasion and intercrown spacing. American Midland Naturalist 112:24–28.

Rodríguez-Iturbe, I., A. Porporato, L. Ridolfi, V. Isham, and D. R. Cox. 1999. Probabilistic modelling of water balance at a point: the role of climate, soil and vegetation. Proceedings of the Royal Society A: Mathematical, Physical and Engineering Sciences 455: 3789–3805.

Shugart, H. H., and D. C. West. 1977. Development of an Appalachian deciduous forest succession model and its application to

assessment of impact of chestnut blight. Journal of Environmental Management 5:161–179.

Stout, B. B. 1956. Studies of the root systems of deciduous trees. Black Rock Forest 15:1–45.

Strigul, N., D. Pristinski, D. Purves, J. Dushoff, and S. Pacala. 2008. Scaling from trees to forests: tractable macroscopic equations for forest dynamics. Ecological Monographs 78:523–545.

Tilman, D. 1988. Plant strategies and the dynamics and structure o plant communities. Princeton University Press, Princeton, NJ.

van Wijk, M. T., and W. Bouten. 2001. Towards understanding tree root profiles: simulating hydrologically optimal strategies for root distribution. Hydrology and Earth System Sciences 5:629–644.

Walter, H., and S.-W. Breckle. 1985. Ecological systems of the geobiosphere. Vol. 1. Ecological principles in global perspective. Springer, Berlin.

Weiner, J., P. Stoll, H. Muller-Landau, and A. Jasentuliyana. 2001. The effects of density, spatial pattern, and competitive symmetry on size variation in simulated plant populations. American Naturalist 158:438–450.

Weltzin, J. F., M. E. Loik, S. Schwinning, D. G. Williams, P. A. Fay, B. M. Haddad, J. Harte, et al. 2003. Assessing the response of terrestrial ecosystems to potential changes in precipitation. BioScience 53:941–952.

Whittaker, R. H. 1975. Communities and ecosystems. 2nd ed. MacMillan, New York.

Woodward, F. I. 1987. Climate and plant distribution. Cambridge University Press, New York.

Zavala, M., and R. Bravo de la Parra. 2005. A mechanistic model of tree competition and facilitation for Mediterranean forests: scaling from leaf physiology to stand dynamics. Ecological Modelling 188: 76–92.

Zea-Cabrera, E., Y. Iwasa, S. Levin, and I. Rodríguez-Iturbe. 2006*a*. Tragedy of the commons in plant water use. Water Resources Research 42:W06D02.

———. 2006*b*. Correction to "Tragedy of the Commons in Plant Water Use." Water Resources Research 42:W09701.

Associate Editor: Frederick R. Adler
Editor: Mark A. McPeek

A closed-canopy forest in Indiana. Photo by Caroline Farrior.

 DOI: 10.1086/669153

Appendix A from C. E. Farrior et al., "Competition for Water and Light in Closed-Canopy Forests: A Tractable Model of Carbon Allocation with Implications for Carbon Sinks"

(Am. Nat., vol. 181, no. 3, p. 000)

Full Model Description with Mathematical Appendixes

Our model may be thought of as a physiologically structured individual-based model with a mechanistic treatment of resource dynamics and a hierarchy of scales. It produces individual trees from physiological and allometric building blocks, competes all possible combinations of the building blocks against one another, and determines the winner(s) as a function of environmental conditions.

In what follows, we first describe the structure of trees and the dependence of photosynthesis on plant traits and resource availability ("Individual Trees"). We then describe the mechanisms of competition for water and light included in the model ("Resource Availability"). Finally, we detail methods of analysis used to solve for competitively dominant, or evolutionarily stable, strategies (ESSs; "Methods of Analysis").

Individual Trees

Tree Structure

The structure of individual trees in our model is governed by species-specific allometric relationships:

$$\begin{aligned} Z &= HD^{\gamma-1}, \\ S &= \alpha_s D^{\gamma+1}, \\ W &= \alpha_w D^{\gamma}. \end{aligned} \tag{A1}$$

Tree height (Z), carbon in structural biomass (S), and the cross-sectional area of the crown of the tree (W) are all functions of the stem diameter (D). Allometric constants H, α_s, and α_w are species specific. A tree with a larger H is taller for a given stem diameter than a tree with a smaller H. Likewise, trees with higher α_s or α_w values have more structural carbon or larger crown areas for a given stem diameter, respectively.

Note that the exponent γ is common to all three of these equations. In this model, we assume that γ is close to 1.5, for reasons explained below, making the scaling exponents for Z, S, and W 0.5, 2.5, and 1.5, respectively. That is, both S and W accelerate with diameter, while Z decelerates with diameter.

Empirical data show that the exponent of the allometric relationship between Z and D is 0.58 (± 0.13 SD), averaged across many species (analysis of U.S. Forest Inventory Analysis data compiled in Lichstein et al. 2010). This exponent is not significantly different from the value we use. The total volume of the wood in a tree can be approximated as a tapered cylinder (McMahon 1973). As a solid of rotation, this volume and thus biomass S scale with Z multiplied by the cross-sectional area of the stem (which scales as D^2). This gives us a value of 2.5 for the scaling of structural biomass with diameter.

Data on trees from 32 states in the Forest Health Monitoring program show that crown area scales with stem diameter to the power of 1.3 (± 0.3 SD) (Woodall et al. 2010). In addition, Lambert et al. (2005) found that tree leaf mass (which our model predicts should scale directly with crown area) scales with stem diameter to the power of 1.66 (± 0.3 SD). Thus, we use a crown area scaling exponent of exactly 1.5 for three reasons: (1) it is a close fit to both empirical relationships; (2) as we see below in "Carbon Allocation and Growth," this value closes the carbon budget in a simple way, greatly increasing the tractability of the model; and (3) if the exponent of the relationship between crown area and diameter were far from 1.5, there would be a persistent acceleration or deceleration in tree size or fecundity, which is not evident in the data (see "Persistent Directional Change in Fecundity and/or Diameter Growth Rate with Allometric Deviations" for further explanation).

Sapwood, the portion of structural biomass that respires, is also described by an allometry. The area of sapwood in a

cross section of a tree has been shown to scale approximately linearly with diameter (Kumagai et al. 2005). In addition, the width of sapwood has been shown to be relatively constant within a tree (Longuetaud et al. 2006). The total volume of sapwood, then, is proportional to the height of the tree multiplied by diameter and is linearly dependent on the number of leaf layers per unit area (sapwood volume $= \alpha_{sw} D^{\gamma} l(t)$). The proportionality constant, α_{sw}, is a species-specific parameter.

Our model remains tractable for values of γ other than 1.5 as long as the relationships among the exponents remain the same (eq. [A1]). Analysis of the model with different relationships among the exponents is still possible but must rely much more heavily on numerical methods.

We assume that tree crowns have flat tops (see fig. A1). This approximation to real crown shapes improves the analytical tractability of our model and in the past has been useful and accurate for predicting the forest dynamics of the lake states of the United States (Purves et al. 2008). Leaves, roots, and reproductive output are also governed by allometric equations:

$$\begin{aligned} \text{total leaf area} &= l(L, \Psi_A)\alpha_w D^{\gamma} = l(L, \Psi_A)W, \\ \text{total fine-root surface area} &= r(L, \Psi_A)\alpha_w D^{\gamma} = r(L, \Psi_A)W, \\ \text{fecundity} &= F(L, \Psi_A)\alpha_w D^{\gamma} = F(L, \Psi_A)W. \end{aligned} \tag{A2}$$

Total leaf area and fine-root surface area scale proportionally with crown area; l is then the leaf area index of the crown, and r is then the fine-root surface area per unit crown area. The root surface area should be proportional to W in order to maintain a sufficient supply of water transpired through the leaves during photosynthesis without overinvesting (see app. A of Dybzinski et al. 2011 for verification of this relationship with several distinct data sets). Trees with higher values of l or r have more leaves or roots, respectively, per unit W. The total fecundity of the tree also scales with crown area. The resource dependencies in equation (A2) on light level (L) and soil-water potential (Ψ_A) allow trees plasticity to respond to changes in resource levels; however, the shapes of the $l(L,\Psi_A)$, $r(L,\Psi_A)$, and $F(L,\Psi_A)$ functions are species specific and are described below.

The collection of possible values of the species-specific parameters and functions H, α_s, α_w, $l(L, \Psi_A)$, $r(L, \Psi_A)$, and $F(L, \Psi_A)$ describe the universe of possible species in this model. It is important to note that we use the term "species" to distinguish sets of trees with differing trait values. In nature, differences in trait values across a landscape sometimes may be achieved by plasticity of a single species. Also, more than one species might express the same set of trait values. Here, we use the term "species" for convenience, although the term may in reality correspond to a single or several species or even to a collection of genotypes within a species.

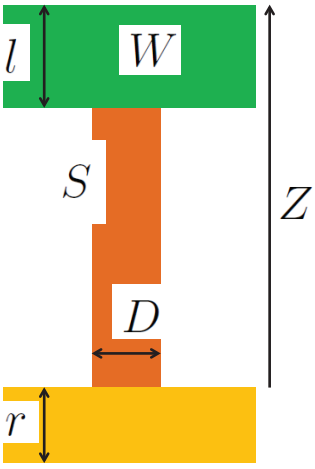

Figure A1: The structure of trees in our model is governed by allometric equations. Crown area ($W = \alpha_w D^{\gamma}$), structural biomass ($S = \alpha_s D^{\gamma+1}$), and height ($Z = HD^{\gamma-1}$) are related directly to stem diameter (D). The total leaf area and root investment are measured per unit W by l and r, respectively. In competition with other trees, this tree may bend its stem to forage for light and distribute its mass of roots throughout the soil (potentially well beyond the drip line of the canopy) to forage for water.

Tree-Level Carbon Assimilation

Our physiological model is designed to maintain analytical tractability while incorporating, at least qualitatively, the most important mechanisms that balance water loss and carbon gain. This model can be derived directly from more complicated physiological models, such as the one used in LM3V (a land-surface vegetation model that is coupled to an atmospheric model; Shevliakova et al. 2009), by making the following simplifying assumptions. First, atmospheric conditions (temperature, humidity, wind speed, and light) are constant over the period of the growing season. The diurnal cycle is approximated by a square wave with constant conditions in the day and in the night. Second, we assume that soil moisture does not vary significantly within 24 h. Typical soil can hold 400 mm, while trees typically transpire at most 4.5 mm in a day (Rodríguez-Iturbe et al. 1999). Finally, we approximate leaf temperature by air temperature. In general, leaf temperature is within a few degrees of air temperature, a fact several useful models rely on (Penman-Monteith equation, analyzed in Paw and Gao 1988). We deal explicitly with precipitation as an environmental variable below, but we can easily use this model to examine changes in temperature, humidity, or solar radiation simply by making explicit the dependence of model parameters (e.g., water-use efficiency and the maximum rate of photosynthesis) on them.

In this model, we assume that water and light are the sole limiting resources. In cases where water is not limiting, we assume that carbon assimilation for a unit of leaf, A_x, increases proportionately with the amount of light incident on the leaf, L, until assimilation reaches a threshold value of V in a unit of leaf area.

$$A_x = \min(\alpha_f L, V). \tag{A3}$$

Carbon assimilation by the whole crown is the integration of A_x through the different leaf layers, which have decreasing levels of light. The light level of a leaf in a tree crown below n leaf layers is approximated by Beer's law, $L = L_X e^{-kn}$, where L_X is the light at the top of the tree's crown. In what follows, we use $L_X = L_0$ for canopy trees and L_U for understory trees. Approximating l as a continuous variable, we find that the total rate of carbon uptake per unit crown area for a tree growing in light level L_X is the integration of A_x through the tree leaf layers:

$$A_L \equiv \begin{cases} Vl & \text{if } 0 < l < \tilde{l}, \\ \dfrac{V}{k}\left(1 + \ln\left(\dfrac{\alpha_f L_X}{V}\right) - \dfrac{\alpha_f L_X}{V} e^{-kl}\right) & \text{if } 0 < \tilde{l} < l, \\ \dfrac{\alpha_f L_X}{k}(1 - e^{-kl}) & \text{if } \tilde{l} < 0 < l, \end{cases} \tag{A4}$$

where $\tilde{l} = (1/k)\ln(\alpha_f L_X/V)$ is the number of leaf layers that operate at the light-saturated photosynthetic rate of V despite self-shading. The first case describes trees in which all of the leaf layers are light saturated. The second case describes trees that have both light-saturated and unsaturated leaf layers. The third case describes trees that have no light-saturated leaf layers, a likely scenario for understory plants.

As plants open their stomates to take in CO_2, water is lost by evaporation. This water is supplied by the roots (rW) at a rate proportional to the gradient of water potential between the xylem and the soil ($\Psi_A - \Psi_X$):

$$\text{water supply} = rWC(\Psi_A - \Psi_X), \tag{A5}$$

where C is the proportionality constant (a conductance).

Here, we assume constant water-use efficiency ω to link the demand for CO_2 to the water loss through stomata,

$$\text{water demand} = \frac{AW}{\omega}, \tag{A6}$$

where A is the photosynthetic rate (A_L from equation [A4] if the tree is water saturated). Water supply and demand must be balanced at all times. The pull on the water supply from leaves changes Ψ_X, increasing the gradient between the water potential of the soil and the tree's xylem until water supply equals water demand:

$$\Psi_X = \Psi_A - \frac{A}{rC\omega}. \tag{A7}$$

It is possible that the demand becomes so high that the Ψ_X needed to meet the demand would damage the tree. When

this happens, we assume that plants can flutter or close their stomata to reduce water demand and keep Ψ_X over a critical value Ψ_C. This also reduces the photosynthetic rate A below A_L, as specified in equation (A6). Thus, if the Ψ_A is high enough that the Ψ_X demanded by A_L is greater than Ψ_C, the tree will be able to assimilate carbon at a rate equal to A_L. Otherwise, trees will be limited by their Ψ_C and assimilate carbon in proportion to the rate at which they can move water, A_W:

$$A = \begin{cases} A_L & \text{if } \Psi_A > \dfrac{A_L}{rC\omega} + \Psi_C, \\ rC\omega(\Psi_A - \Psi_C) \equiv A_W & \text{otherwise.} \end{cases} \tag{A8}$$

To see an illustration of the dependence of Ψ_X and A on Ψ_A, a measure of water available to the tree, refer to figure A2.

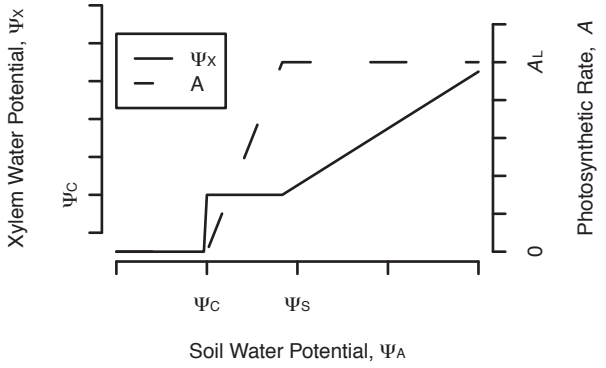

Figure A2: Physiology of water limitation in the model. When plants are water limited ($\Psi_C < \Psi_A < \Psi_S$), photosynthetic rate (A, defined as carbon fixation per unit crown area of a tree per year) increases with water availability, as trees hold their xylem at the lowest possible water potential ($\Psi_X = \Psi_C$). When plants are water saturated ($\Psi_A > \Psi_S$), photosynthetic rate is determined by light availability and soil water no longer influences photosynthesis. When soil water drops lower than the minimum water potential of the plants ($\Psi_A < \Psi_C$), xylem cavitates, no photosynthesis occurs, and the plant dies.

Carbon Allocation and Growth

Carbon assimilated over the year is allocated by the tree to replace dropped leaves and dead fine roots; to build additional leaves and fine roots; for respiration of fine roots, leaves, and sapwood; to grow in stem biomass; and to produce offspring. We begin by describing the yearly average rates of all movements of carbon into, out of, and within the tree.

Carbon uptake is proportional to the crown area of the tree,

$$\text{rate of carbon fixation} = W(t)A(t). \tag{A9}$$

Carbon inputs to tree structure are as follows:

$$\begin{aligned}
\text{replacement of dropped leaves} &= W(t)l(t)\frac{c_{\text{l,b}}}{\tau_{\text{l}}},\\
\text{replacement of dead roots} &= W(t)r(t)\frac{c_{\text{r,b}}}{\tau_{\text{r}}},\\
\text{growth of leaf mass} &= \left(l(t)\frac{dW}{dt} + \frac{dl}{dt}W(t)\right)c_{\text{l,b}},\\
\text{growth of fine-root surface area} &= \left(r(t)\frac{dW}{dt} + \frac{dr}{dt}W(t)\right)c_{\text{r,b}},\\
\text{stem growth} &= \frac{dS}{dt},\\
\text{fecundity} &= W(t)c_{\text{f}}F(t).
\end{aligned} \tag{A10}$$

Similarly, outputs from the tree's structure are

$$\begin{aligned}
\text{fine-root respiration} &= p_{\text{r}}r(t)W(t),\\
\text{leaf respiration} &= p_{\text{l}}l(t)W(t),\\
\text{sapwood respiration} &= p_{\text{sw}}\alpha_{\text{sw}}D^{\gamma}l(t),
\end{aligned} \tag{A11}$$

where $c_{\text{l,b}}$ is the cost of building a unit of leaf in carbon, $c_{\text{r,b}}$ is the cost of building a unit of fine-root surface area in carbon, τ_{l} and τ_{r} are the average lifetimes of a unit of carbon in leaves and roots, respectively, c_{f} is the carbon cost per individual offspring produced by the tree, F is the fecundity per unit W, and p_{l}, p_{r}, and p_{sw} are the respiration rates of leaves, fine roots, and sapwood, respectively. Because respiration rates are functions of temperature in nature, p_{l}, p_{r}, and p_{sw} should be thought of as time averages in a constant climate.

Because carbon atoms are conserved, the rate of carbon assimilation must equal the rate of carbon allocated to the various plant organs:

$$\begin{aligned}
W(t)A(t) = {} & W(t)l(t)\frac{c_{\text{l,b}}}{\tau_{\text{l}}} + W(t)r(t)\frac{c_{\text{r,b}}}{\tau_{\text{r}}} + l(t)\frac{dW}{dt}c_{\text{l,b}} + W(t)\frac{dl}{dt}c_{\text{l,b}} + r(t)\frac{dW}{dt}c_{\text{r,b}} + W(t)\frac{dr}{dt}c_{\text{r,b}}\\
& + l(t)W(t)p_{\text{l}} + r(t)W(t)p_{\text{r}} + \alpha_{\text{sw}}D(t)^{\gamma}p_{\text{sw}}l(t) + \frac{dS}{dt} + W(t)c_{\text{f}}F(t).
\end{aligned} \tag{A12}$$

Using the allometric relationships $W = \alpha_{\text{w}}D^{\gamma}$ and $S = \alpha_{\text{s}}D^{\gamma+1}$ (eq. [A1]), we can rearrange equation (A12) to solve for dD/dt,

$$\frac{dD}{dt} = \frac{1}{[\alpha_{\text{s}}(\gamma+1)(1+c_{\text{b,g}})/\alpha_{\text{w}}] + (\gamma/D)(lc_{\text{l,b}} + rc_{\text{r,b}})}\left(A - lc_{\text{l}} - rc_{\text{r}} - \frac{dl}{dt}c_{\text{l,b}} - \frac{dr}{dt}c_{\text{r,b}} - c_{\text{f}}F\right), \tag{A13}$$

where $c_{\text{l}} = (c_{\text{l,b}}/\tau_{\text{l}}) + p_{\text{l}} + p_{\text{sw}}(\alpha_{\text{sw}}/\alpha_{\text{w}})$ and $c_{\text{r}} = (c_{\text{r,b}}/\tau_{\text{r}}) + p_{\text{r}}$. We note here that in this step we were able to cancel much of the dependence of the growth rate on diameter. This is crucial for tractability and is owed to our empirically supported assumptions about the relationships among the allometric exponents, described in "Tree Structure." In addition, we note that as diameter increases, the growth rate can be approximated as

$$\frac{dD}{dt} \approx \frac{\alpha_{\text{w}}}{\alpha_{\text{s}}(\gamma+1)(1+c_{\text{b,g}})}\left(A - lc_{\text{l}} - rc_{\text{r}} - \frac{dl}{dt}c_{\text{l,b}} - \frac{dr}{dt}c_{\text{r,b}} - c_{\text{f}}F\right), \tag{A14}$$

removing all dependence on diameter. We confirm in "Diameter Growth as Independent of Diameter" the result of Dybzinski et al. (2011) that the omitted term in equation (A14) has a negligible impact on lifetime reproductive success (LRS), the critical value used for predictions of this model (defined below).

Resource Availability

The level of resources available to a single tree is the result of both resource input and competition. The downward flux of light at the top of the canopy, L_0, comes in from directly overhead, and a constant drizzle of rain, R, wets the soil. Trees cast shade and take up water, potentially lowering both resource levels before they reach a focal tree.

Light Availability

The shade cast by a closed canopy is approximated by a modified Beer's law,

$$L_U = L_0 e^{-xk\bar{l}}, \tag{A15}$$

where $\bar{l}$ is the canopy's average number of leaf layers and x is a constant between 0 and 1 that accounts for sunflecks caused by movement of trees in the wind and damage to the canopy. Most individual-based forest models use full spatial simulators of all trees in a forest to determine the number of leaves shading a given tree. Recent advances have shown that using the assumption that trees are perfectly plastic in their horizontal foraging for light (the "perfect-plasticity approximation" [PPA]) is a good analytical approximation to full spatial simulators of forests where trees have tessellating crowns and especially if they have even a small ability to bend toward light (Purves et al. 2007; Strigul et al. 2008). A model using this assumption has been shown to be accurate for predictions of forest succession in the lake states of the United States (Purves et al. 2008). We take advantage of these advances and include the PPA in our model.

The assumptions behind the PPA imply that a forest canopy is filled by the crowns of the tallest trees present and that canopy trees do not shade one another. Crowns beneath the canopy layer also efficiently partition space and also do not shade one another, unless a second layer is filled, in which case, the first two canopy layers shade a third composed of still shorter trees. In this article, the parameter values used produce only stands with one full layer and one partial understory layer.

We define Z^* as the height of the shortest canopy tree. In such a forest, all trees taller than Z^* are in direct sunlight (L_0), while shorter trees are shaded uniformly by a layer of canopy trees and experience light levels given by equation (A15).

Water Availability

The rate of change of plant-available water in the soil, θ, is dependent on the incoming rate of rainfall and the rate of uptake by trees. We assume that matric forces of the soil are negligible, such that both rainfall input and tree uptake are well mixed. The soil has a maximum water-holding capacity θ_B and a corresponding soil-water potential Ψ_B,

$$\frac{d\theta}{dt} = \begin{cases} R - \int_0^\infty W(x)\frac{A(x)}{\omega}N(x)dx & \text{if } \theta < \theta_B, \\ 0 & \text{if } \theta = \theta_B, \end{cases} \tag{A16}$$

where $N(x)$ is the density of trees of size x. Under constant rate of rainfall R, θ will equilibrate at a level determined by setting the first equation to 0 if trees are water limited or will reach θ_B if trees are water saturated. The relationship between water potential and the volume of water taken up by a unit of root can be complicated, but over a wide range of conditions it is approximately linear. Thus, we treat conductance C in equation (A8) as a constant.

In summary, all trees in a monoculture (with a closed canopy and an incomplete subcanopy) have a total of two possible resource levels in the model at any given time. Trees in the canopy have light level L_0 at the top of their crowns, whereas those in the understory have light level given by equation (A15). All trees, canopy or understory, experience the same water availability at a given time.

Now imagine equilibrium conditions, where Ψ_A, L_U, and Z^* are constant. The only difference in resource availability that a tree experiences throughout its life is when it moves from light level L_U to L_0, that is, when it grows into the canopy as its height passes Z^*. Thus, a monoculture stand has at most two different types of resource levels, each with single values of resource-dependent functions l, r, F, and G. From here on we use "c" and "u" as subscripts to denote the

canopy and understory values, respectively, of these functions. We assume that $F_u = 0$ in our analysis, a good approximation for trees. In addition, we assume that mortality is a function of plant strategy and resource availability (not explicitly a function of age or size), making two possible mortality extinction coefficients, μ_c and μ_u.

For the moment, assume that the only time that leaf and root investment changes is when the tree enters the canopy at height Z^* and resource availability changes. As we see below, these strategies outcompete other strategies. Because l and r have fast dynamics relative to the diameter growth (see "Timescale of Transition to Canopy Leaf Area Index and Root Area Index"), we can obtain an accurate approximation by assuming that l and r adjust instantaneously from their understory equilibrium values to the canopy equilibrium values as the tree crosses into the canopy. This makes sense intuitively because the entire leaf and root masses of a deciduous canopy tree represent about 2 years of net primary production. In contrast, 2 years of production will change the diameter of a canopy tree by only a few percent. Using the approximation that dl/dt and dr/dt are 0 in the conservation equation gives us the stem growth equations for the canopy and the understory:

$$G_c = \frac{dD}{dt} \approx \frac{\alpha_w}{\alpha_s(\gamma + 1)(1 + c_{b,g})}(A_c - c_l l_c - c_r r_c - c_f F_c),$$

$$G_u = \frac{dD}{dt} \approx \frac{\alpha_w}{\alpha_s(\gamma + 1)(1 + c_{b,g})}(A_u - c_l l_u - c_r r_u). \tag{A17}$$

The simplified growth equation allows us to take advantage of a particularly tractable version of the PPA model with diameter-independent but resource- and trait-dependent growth rates.

With this framework, we have constant understory and canopy growth and mortality rates with respect to environmental conditions, and we now use the PPA to scale from individual vital rates to competitive dynamics. The critical value for this is the height of canopy closure for a monoculture, Z^* (Adams et al. 2007). From the solution to the von Foerster equations found in Strigul et al. (2008) for flat-top trees with an arbitrary crown area to diameter scaling (see "Z^* Derivation"), this height is

$$\hat{Z}^* = H(\hat{D}^*)^{\gamma-1} \approx H\left(\frac{G_u}{\mu_u}\ln\left(\frac{F_c\alpha_w\Gamma(\gamma + 1)G_c^\gamma}{\mu_c^{\gamma+1}}\right)\right)^{\gamma-1}, \tag{A18}$$

where Γ is the gamma function. Because Z^* determines the amount of time that an individual will spend at understory vital rates, it is important in competition. The value increases with growth rates and fecundity, decreases with mortality, and is dependent on the allometric constants of our trees.

Methods of Analysis

With the model we have described, we can easily derive a number of properties of a monoculture stand at equilibrium that will prove useful for the calculation of dominant strategies that can competitively exclude other strategies.

Equilibrium Stand Properties: Closed-Canopy Criterion

First, we derive the closed-canopy criterion. For a species to have a closed-canopy stand at equilibrium, at the very least, the total crown area of all trees of the species, if they were grown in the open, must be greater than the ground area (P):

$$P < \int_0^\infty F_c P e^{-\mu_c \tau}\alpha_w(G_c\tau)^\gamma d\tau, \tag{A19}$$

or equivalently,

$$1 < F_c\alpha_w\frac{G_c^\gamma}{\mu_c^{\gamma+1}}\Gamma(\gamma + 1). \tag{A20}$$

Equilibrium Stand Properties: Understory Crown Area

In a monoculture at equilibrium, the total area covered by crowns of the understory is dependent on the input of new trees produced by the canopy (F_c) and the growth and mortality of those trees before they reach the canopy at diameter $\hat{D}^*$,

$$\begin{aligned}\hat{U} &= F_c P \int_0^{\hat{D}^*/G_u} e^{-\mu_u t} \alpha_w (G_u t)^\gamma dt \\ &= \frac{F_c P \alpha_w G_u^\gamma}{\mu_u^{\gamma+1}} \left[\Gamma(\gamma+1) - \Gamma\left(\gamma+1, \frac{\mu_u}{G_u}\hat{D}^*\right)\right], \end{aligned} \tag{A21}$$

where $\hat{U}$ is the equilibrium total understory crown area and t is the age of trees.

Equilibrium Stand Properties: Gross Primary Production, Net Primary Production, and Carbon Storage

The productivity of a closed-canopy stand can also be calculated from our framework. If we use A_u to indicate the rate of carbon uptake per unit tree-crown area for the understory resource levels ($A(\hat{L}_U, \hat{\Psi}_A, l_u, r_u)$) and A_c to indicate the carbon uptake per unit tree-crown area for canopy resource levels ($A(L_0, \hat{\Psi}_A, l_c, r_c)$; see eq. [A8]), then the gross primary productivity ($\hat{\text{GPP}}$, kg C m^{-2} yr^{-1}) of the total forest at equilibrium can be expressed as

$$\hat{\text{GPP}} = A_c P + A_u \hat{U} \approx A_c P. \tag{A22}$$

The understory contribution to the GPP is negligible compared to that of the canopy for most cases, as both $\hat{U}$ and A_u are almost always much smaller than P and A_c. Therefore, $A_c P$ is a good approximation for $\hat{\text{GPP}}$.

The net primary productivity of a stand at equilibrium ($\hat{\text{NPP}}$, kg C m^{-2} yr^{-1}), a more easily measurable stand property, can also be derived from the model. The NPP is simply the GPP minus the costs of leaf, sapwood, and fine-root respiration. Again, the canopy components are a good approximation of the total NPP:

$$\begin{aligned}\hat{\text{NPP}} &= A_c - \left(p_l + p_{sw}\frac{\alpha_{sw}}{\alpha_w}\right) l_c - p_r r_c + \left[A_u - \left(p_l + p_{sw}\frac{\alpha_{sw}}{\alpha_w}\right) l_u - p_r r_u\right]\hat{U} \\ &\approx A_c - p_l l_c - p_r r_c. \end{aligned} \tag{A23}$$

This $\hat{\text{NPP}}$ can be divided into foliage, fine roots, and structural biomass, which will be useful in comparing model predictions with data:

$$\begin{aligned}\hat{\text{NPP}} &= \text{foliage NPP} + \text{root NPP} + \text{structural biomass NPP} \\ &\approx l_c \frac{c_{l,b}}{\tau_l} + r_c \frac{c_{r,b}}{\tau_r} + \frac{\alpha_s(\gamma+1)}{\alpha_w} G_c. \end{aligned} \tag{A24}$$

The total carbon stored in live biomass (kg C m^{-2}) of a monoculture at equilibrium is the sum of carbon stored in woody biomass, leaves, and fine roots,

$$\begin{aligned}\hat{\text{carbon storage}} &= \text{structural biomass} + \text{leaf biomass} + \text{fine-root biomass} \\ &\approx \text{canopy structural biomass} + l_c \text{LMA} + r_c \text{RMA}, \end{aligned} \tag{A25}$$

where LMA and RMA are the mass in kilograms of carbon per unit area of leaves and fine roots, respectively. Canopy structural biomass is the structural biomass per tree times the density of trees of that size,

$$\begin{aligned}\text{canopy structural biomass} &= \int_0^\infty \alpha_s (D^* + G_c\tau)^{\gamma+1} F_c e^{-(\mu_u/G_u)D^* - \mu_c\tau} d\tau \\ &\approx \frac{\alpha_s(\gamma+1)}{\alpha_w}\frac{G_c}{\mu_c},\end{aligned} \tag{A26}$$

using the approximation that $(\mu_c/G_c)D^* \ll (\gamma + 1)$.

Equilibrium Stand Properties: Stability Criteria

To find the competitively dominant strategies by successive invasions of monocultures at equilibrium with adaptive-dynamics analyses, it is necessary that the size distribution, the height of canopy closure, the understory light level, and the water potential are all stable equilibria. That is, if we added a few trees or cut down a few trees from a steady state forest, that forest would return to the same equilibrium size distribution. These properties are stable if the plant strategy and environment allow a closed canopy (see criterion in eq. [A20]) and the growth rate of the understory in monoculture is greater than 0. See "Stability of the Dynamic Equilibrium" for a proof of these conditions. In this article, we restrict our analyses to cases where these conditions are met.

Predicting Dominant Plant Strategies

We use adaptive-dynamics analyses to predict the outcome of species interactions and, ultimately, community composition (Geritz et al. 1998; McGill and Brown 2007). We calculate the ability of different plant strategies to invade a monoculture at equilibrium. This will allow us to find uninvadable plant strategies if they exist.

We use the expected lifetime reproductive success (LRS, a measure of fitness) of an invading species (I) with a negligible population size experiencing resource availability set by environmental inputs and the resource uptake of the resident species (R) at its monoculture equilibrium as a measure of invasion potential:

$$\begin{aligned}\mathrm{LRS}(I,R) &= e^{-\mu_u(I,R)(D^*_{R,I}/G_u(I,R))} \int_0^\infty e^{-\mu_c(I,R)\tau} F_c(I,R)\alpha_{w,I}(D^*_{R,I} + G_c(I,R)\tau)^\gamma d\tau \\ &\approx F_c(I,R)\alpha_{w,I}\Gamma(\gamma+1)\frac{G_c(I,R)^\gamma}{\mu_c(I,R)^{\gamma+1}} e^{-(\mu_u(I,R)/G_u(I,R))D^*_{R,I}},\end{aligned} \tag{A27}$$

where $D^*_{R,I} = (H_R/H_I)^{1/(\gamma-1)}D^*_R$, or the diameter at which species I trees would be tall enough (Z^*_R) to enter the canopy of a forest filled with trees of species R. The term $G_c(I, R)$ indicates the diameter growth rate of trees of species I in the resource availability set by trees of species R, and the notational convention holds for other vital rates.

The LRS is the sum of the fecundity of a tree for a stage multiplied by the probability that the tree will reach that stage. The term outside the integral is the probability that a seedling will reach the canopy, the stage at which trees begin reproducing. Note that $D^*_{R,I}/G_u(I, R)$ is the time required to reach the canopy, given negligible initial diameter. The integrand is the fecundity rate of an individual that has spent τ years in the canopy and the probability that the individual will be alive at that point, $e^{-\mu_c(I,R)\tau}$. Recall that F_c is defined per unit crown area and thus is multiplied by crown area to find an individual's total fecundity. The solution of the integral is derived from the same approximations as those used for Z^* (see "Z^* Derivation").

It can easily be shown that if species I is the same as species R, then the LRS is equal to 1. Appropriately, at equilibrium, an individual has an expectation of producing one individual to replace itself over its lifetime. Now consider two species, j and k. If $\mathrm{LRS}(j, k) > 1$, then j can increase from rarity in a near monoculture of species k.

If a strategy k^{ESS} is an evolutionarily stable strategy, there should be no other strategy in all of strategy space that

satisfies the invasion criterion. Thus, if an ESS (k^{ESS}) exists, it can be found by satisfying the following criteria, adapted directly from Maynard Smith and Price (1973):

$$\begin{aligned} &\mathrm{LRS}(j, k^{\mathrm{ESS}}) < 1 \text{ or} \\ &\mathrm{LRS}(j, k^{\mathrm{ESS}}) = 1 \text{ and } \mathrm{LRS}(k^{\mathrm{ESS}}, j) > 1, \end{aligned} \tag{A28}$$

for all j not equal to k^{ESS}.

In practice, we find local ESSs, which are uninvadable by nearby strategies, and check that they are convergence stable analytically. We then check whether these local ESSs are uninvadable by all strategies in the space of viable tree strategies numerically. Pairwise invasion plots generated from these numerical evaluations are presented in figure 1 and the figures of appendix C. The following is the color key for these diagrams, where j is the "green strategy" and k is the "blue strategy":

$$\begin{aligned} \text{Green} \quad & \mathrm{LRS}(j, k) > 1 \text{ and } \mathrm{LRS}(k, j) < 1, \\ \text{Blue} \quad & \mathrm{LRS}(j, k) < 1 \text{ and } \mathrm{LRS}(k, j) > 1, \\ \text{Yellow} \quad & \mathrm{LRS}(j, k) > 1 \text{ and } \mathrm{LRS}(k, j) > 1, \\ \text{Black} \quad & D^{*}(k, k) < 0. \end{aligned} \tag{A29}$$

Mathematical Appendixes to the Model Description

Persistent Directional Change in Fecundity and/or Diameter Growth Rate with Allometric Deviations

In the main text of the article, we have assumed that the exponents of crown area and structural biomass allometry differ by exactly 1. That is, $W = \alpha_{\mathrm{w}} D^{\gamma}$ and $S = \alpha_{\mathrm{s}} D^{\gamma+1}$. Here, we investigate the effect of small deviations in this relationship, where $W = \alpha_{\mathrm{w}} D^{\theta}$ and $S = \alpha_{\mathrm{s}} D^{\gamma+1}$.

The carbon balance equation for the whole tree, in its simplified form (eq. [A17]) with potential differences between θ and γ, becomes

$$WA = Wlc_{\mathrm{l}} + Wrc_{\mathrm{r}} + \alpha_{\mathrm{s}}(\gamma + 1)(1 + c_{\mathrm{b,g}}) D^{\gamma} \frac{dD}{dt} + Wc_{\mathrm{f}} F, \tag{A30}$$

and it may be simplified to

$$A = lc_{\mathrm{l}} + rc_{\mathrm{r}} + \frac{\alpha_{\mathrm{s}}(\gamma + 1)(1 + c_{\mathrm{b,g}})}{\alpha_{\mathrm{w}}} D^{\gamma-\theta} \frac{dD}{dt} + c_{\mathrm{f}} F. \tag{A31}$$

If θ and γ are different, then either F or dD/dt must change as trees grow in diameter to maintain conservation of carbon. If F, the fecundity per unit crown area, changes but dD/dt does not ($D(t) = D(0) + t(dD/dt)$), then we find

$$F(t) = \frac{1}{c_{\mathrm{f}}} \left[A - lc_{\mathrm{l}} - rc_{\mathrm{r}} - \frac{\alpha_{\mathrm{s}}(\gamma + 1)(1 + c_{\mathrm{b,g}})}{\alpha_{\mathrm{w}}} \frac{dD}{dt} D(t)^{\gamma-\theta} \right]. \tag{A32}$$

As diameter grows, the fecundity output per unit crown area continues to increase or decrease if θ is greater than or less than γ, respectively. With the default parameter values in table A1 and $A = 2$ kg C m^{-2} year^{-1}, a 0.2 deviation of θ from γ necessitates a 24% decrease (if $\gamma = 1.5$ and $\theta = 1.3$) or a 4% increase (if $\gamma = 1.5$ and $\theta = 1.7$) in fecundity as trees grow from 12 to 24 cm in diameter.

Conversely, if $\theta \neq \gamma$ and fecundity is constant, then the diameter growth rate must change as the diameter itself grows:

$$\frac{dD}{dt}(t) = \frac{\alpha_{\mathrm{w}}}{\alpha_{\mathrm{s}}(\gamma + 1)(1 + c_{\mathrm{b,g}})} (A - lc_{\mathrm{l}} - rc_{\mathrm{r}} - c_{\mathrm{f}} F) D^{\theta-\gamma}. \tag{A33}$$

Using the fact that $D(0) = 0$, we solve the differential equation and take the derivative to find the dependence of growth rate on time:

$$\frac{dD}{dt} = X[(\gamma - \theta + 1)Xt]^{(\theta-\gamma)/(\gamma-\theta+1)}, \tag{A34}$$

where $X = \{\alpha_w/[\alpha_s(\gamma + 1)(1 + c_{b,g})]\}(A - lc_l - rc_r - c_f F)$. So there are persistent increases or decreases in diameter growth rate if $\gamma \neq \theta$. For example, if θ is less than or greater than γ by 0.2, there must be a compensatory 8% decrease or increase in diameter growth rate, respectively, as the trees grow from 12 to 24 cm in diameter. This percentage only continues to increase as the tree grows further.

Table A1. Frequently used variables

Variable	Description	Units	Estimate
Tree measurements:			
D	Diameter at breast height	cm	
Z	Tree height	m	
S	Total structural biomass	kg C	
W	Crown area	m^2	
G	Diameter growth rate	cm $year^{-1}$	$G_c = .6$;[a] $G_u = .2$[a]
μ	Mortality rate	$year^{-1}$	$\mu_c = .016$; $\mu_u = .038$
F	Fecundity	saplings m^{-2} $year^{-1}$	$F_c = .0071$; $F_u = 0$
l	Leaf area index	m^2 m^{-2}	$l_c = 4$;[a] $l_u = 1$[a]
r	Fine-root surface area	m^2 m^{-2}	$r_c = 6.5$;[a] $r_u = 2$[a]
H	Allometric constant ($Z = HD^{\gamma-1}$)	$m/cm^{\gamma-1}$	3.6
α_w	Allometric constant ($W = \alpha_w D^{\gamma}$)	m^2/cm^{γ}	.20
α_s	Allometric constant ($S = \alpha_s D^{\gamma+1}$)	kg $C/cm^{\gamma+1}$	.0815
γ	Allometric exponent		1.5
c	Subscript indicating a canopy tree's trait		
u	Subscript indicating an understory tree's trait		
Carbon assimilation and allocation:			
A	Plant level carbon assimilation rate per unit crown area	kg C m^{-2} $year^{-1}$	
c_l	Cost of building and maintaining leaf biomass including sapwood respiration	kg C m^{-2} $year^{-1}$	.187
c_r	Cost of building and maintaining fine-root biomass	kg C m^{-2} $year^{-1}$	.044
c_f	Cost of fecundity	kg C $sapling^{-1}$	4.87
$c_{b,g}$	Building cost of structural biomass	kg C (kg C)$^{-1}$	.2
Water-saturated photosynthesis:			
L_0, L_U	Light above the crowns of all trees and of understory trees, respectively	MJ PAR m^{-2} $year^{-1}$	$L_0 = 1{,}200$; $L_U = 446$[a]
k	Light extinction constant (Beer's law)		.33
x	Effective proportion of canopy leaves shading the understory		.75
α_f	Relationship between carbon fixation and light intensity	kg C (MJ PAR)$^{-1}$	.001
V	Maximal rate of carbon fixation	kg C m^{-2} $year^{-1}$	.6
Water-limited photosynthesis:			
R_{wet}, R_{dry}	Rainfall rate of wet and dry days, respectively	m $year^{-1}$	$R_{wet} = 1.5$; $R_{dry} = .75$[a]
q	Proportion of time in water saturation		.6
C	Water conductance through the plant, from soil to leaf	m MPa^{-1} m^{-2} $year^{-1}$	.29
ω	Water-use efficiency	kg C m^{-1}	2
Ψ_C	Critical xylem water potential	MPa	−2.5
Ψ_A	Water availability, in water potential	MPa	

Note: All variables are described at their first use in the main text. Estimates are used as default numbers for simulations and figures drawn. The sources of these estimates from can be found in table A2. PAR = photosynthetically active radiation.

[a]Default values used only when not calculated in the model or specifically varied as an input.

Diameter Growth as Independent of Diameter

Diameter growth is the increase in diameter due to an increase in structural biomass. Equation (A13) describes the growth rate as it is dependent on the tree's allocation to leaves, roots, and fecundity:

$$\frac{dD}{dt} = \frac{1}{[\alpha_s(\gamma + 1)(1 + c_{b,g})/\alpha_w] + (\gamma/D)(lc_{l,b} + rc_{r,b})}\left(A - lc_l - rc_r - \frac{dl}{dt}c_{l,b} - \frac{dr}{dt}c_{r,b} - c_f F\right). \tag{A35}$$

As diameter increases, the growth rate can be approximated as

$$\frac{dD}{dt} \approx \frac{\alpha_w}{\alpha_s(\gamma + 1)(1 + c_{b,g})}\left(A - lc_l - rc_r - \frac{dl}{dt}c_{l,b} - \frac{dr}{dt}c_{r,b} - c_f F\right), \tag{A36}$$

which does not depend on D. This independence from D allows us to take advantage of the perfect-plasticity approximation (Strigul et al. 2008).

By neglecting the diameter term of the right-hand side, we overestimate the growth rate for trees, particularly small ones, making this approximation worse for understory trees (fig. A3). Overestimating the understory growth rate not only decreases the time it takes for a tree to reach a given size but also increases the height of canopy closure. When the lifetime reproductive success of a strategy (our measure of "fitness" and determinant of dominant strategies) is computed, understory growth is used only to calculate the total time that it takes for a tree to make it to the canopy; see equation (A27).

The time that it takes for trees to reach the canopy is D^*/G_u, which is independent of G_u.

$$\frac{D^*}{G_u} = \frac{1}{\mu_u}\ln\left(\frac{F\alpha_w G_c^\gamma \Gamma(\gamma + 1)}{\mu_c^{\gamma+1}}\right). \tag{A37}$$

Thus, for analyses of the competitively dominant strategy for canopy traits, which we focus on, this error has no effect. This error may be important in determining the dominant allocation strategies of very small plants, however. See appendix B of Dybzinski et al. (2011) for a demonstration of the potential size of these errors.

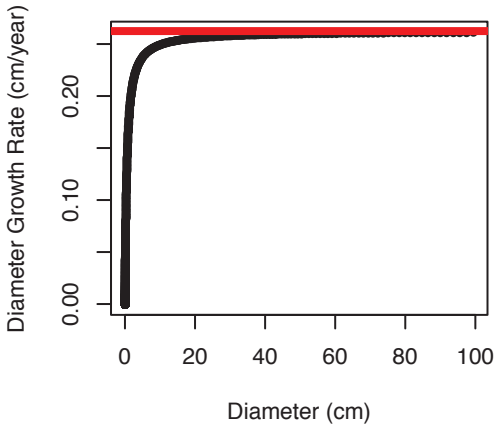

Figure A3: Comparison of the full diameter-dependent growth rate, equation (A35) (black line), with the diameter-independent growth rate approximation, equation (A36) (red line). Parameter estimates can be found in table A1. For this simulation, we used the evolutionarily stable canopy-tree strategies for an environment with $q = 0.5$ and $R_{dry} = 0.8$ (case 3) and the results of "Timescale of Transition to Canopy Leaf Area Index and Root Area Index" ($dl/dt = dr/dt = 0$).

Timescale of Transition to Canopy Leaf Area Index and Root Area Index

At the instant a tree grows out of the understory and into the canopy, it experiences higher light levels. This new

environment may change the individual's strategies of leaf layers and root surface area per unit crown area (l and r, respectively) dramatically. Usually, a tree is able to build leaves and roots every year, using some of the carbon that it used to build them the year before. Building new leaves and roots beyond replacing those that were already held is costly to the tree. Building new structures is different from replacing old ones because there is no carbon to reuse. So when l and r are changing, carbon allocation is different from that in years when they do not change. We show below, however, that it is not common for this change to have a significant impact on the lifetime reproductive success of a tree, and it may be ignored without introducing significant errors in analyses of a model for competitive tree strategies.

As soon as a tree moves from the understory to the canopy, diameter growth does not immediately become G_c, both because the tree does not have full r_c and l_c yet and because it is spending carbon to grow leaf and root layers. During this time,

$$\frac{dD}{dt} \approx \frac{\alpha_w}{\alpha_s(\gamma+1)(1+c_{b,g})}\left(A - lc_l - rc_r - \frac{dl}{dt}c_{l,b} - \frac{dr}{dt}c_{r,b} - c_f F\right). \tag{A38}$$

Here, we determine how long this period of time could be and what effect that has on lifetime reproductive success, the focal measure of this model.

Unless mortality rates are extremely high, a competitive tree should allocate all of its new carbon gained toward increasing its leaves and roots until they have reached the new levels. If mortality is extremely high, it may be advantageous in terms of LRS to allocate carbon toward fecundity completely, but we do not consider these cases here. Then,

$$\begin{aligned} F(t) &= 0, \\ G(t) &= G_u, \end{aligned} \tag{A39}$$

for $0 < t < t_L$, where $t = 0$ when the trees enter the canopy and $t = t_L$ when they are capable of maintaining canopy growth and fecundity:

$$\begin{aligned} l(0) &= l_u, \\ l(t \geq t_L) &= l_c, \\ r(0) &= r_u, \\ r(t \geq t_L) &= r_c, \\ D(0) &= D^*, \\ D(t_L) &= D^* + t_L G_u, \\ D(t \geq t_L) &= D^* + t_L G_u + (t - t_L)G_c. \end{aligned} \tag{A40}$$

The expected lifetime reproductive success of this tree is

$$\mathrm{LRS} = e^{-[(\mu_u/G_u)D^* + \mu_c t_L]} \int_0^\infty e^{-\mu_c \tau} F_c \alpha_w (D^* + G_u t_L + G_c \tau)^\gamma d\tau. \tag{A41}$$

By the same approximations listed in "Z^* Derivation,"

$$\mathrm{LRS} \approx F_c \alpha_w \Gamma(\gamma+1) \frac{G_c^\gamma}{\mu_c^{\gamma+1}} e^{-[(\mu_u/G_u)D^* - (\mu_c/G_c)(D^* + G_u t_L) - \mu_c t_L]}. \tag{A42}$$

How long is t_L? If a tree is competitive, it should be near colimitation in most cases, as is shown in "Results." If a tree is near colimitation as an understory tree, then when it first moves into the canopy, receiving far greater light with the same amount of leaves and fine roots, it should become water limited. To regain colimitation, the tree should immediately

invest all additional carbon gained to increasing fine-root biomass. We call the time when the tree first becomes colimited t_x and the roots it needs to achieve colimitation r_x:

$$r_x C\omega(\Psi_A - \Psi_C) = A_L(L_0, l_u). \tag{A43}$$

Note that we do not consider the effects of changing root values on Ψ_A, because this is a property determined by the whole community of trees, the majority of which are not going through this transition. The carbon balance equation, equation (A12), can be solved for dr/dt in terms of t and r where $dl/dt = 0$:

$$\frac{dr}{dt} = \frac{1}{c_{r,b}}\left[r(t)C\omega(\Psi_A - \Psi_C) - l_u c_l - r(t)c_r - \frac{\alpha_s(\gamma + 1)}{\alpha_w}G_u\right]. \tag{A44}$$

Solving the differential equation for $r(t)$, we find

$$r(t) = \frac{l_u c_l + [\alpha_s(\gamma + 1)/\alpha_w]G_u}{C\omega(\Psi_A - \Psi_C) - c_r} + \left\{r_u - \frac{l_u c_l + [\alpha_s(\gamma + 1)/\alpha_w]G_u}{C\omega(\Psi_A - \Psi_C) - c_r}\right\}e^{\{[C\omega(\Psi_A - \Psi_C) - c_r]/c_{r,b}\}t} \tag{A45}$$

for $0 < t < t_x$ and

$$t_x = \frac{c_{r,b}}{C\omega(\Psi_A - \Psi_C) - c_r}\ln\left(\frac{r_x C\omega(\Psi_A - \Psi_C) - l_u c_l - r_x c_r - [\alpha_s(\gamma + 1)/\alpha_w]G_u}{r_u C\omega(\Psi_A - \Psi_C) - l_u c_l - r_u c_r - [\alpha_s(\gamma + 1)/\alpha_w]G_u}\right). \tag{A46}$$

After the roots have caught up to the leaves, competitive trees begin to allocate carbon to building new leaves and roots in such a way that they will remain colimited until they have built their canopy targets, r_c and l_c. Colimitation is shown to be the competitively dominant strategy in "Resolution to the Paradox of the Tragedy of the Commons for Water Use in Plants": for $t_x < t < t_L$,

$$C\omega r(t)(\Psi_A - \Psi_C) = A_L(L_0, l(t)). \tag{A47}$$

Substituting $r(l)$ into the carbon conservation equation and solving for dl/dt, we find

$$\frac{dl}{dt} = \frac{1}{c_{l,b} + [V/C\omega(\Psi_A - \Psi_C)]c_{r,b}}\left[Vl - lc_l - \frac{Vl}{\omega C(\Psi_A - \Psi_C)}c_r - \frac{\alpha_s(\gamma + 1)}{\alpha_w}G_u\right] \tag{A48}$$

when $l < l^{\sim}$ (see eq. [A4]), and

$$\begin{aligned}\frac{dl}{dt} = {} & \frac{1}{c_{l,b} + [\alpha_f L_0 e^{-kl}/C\omega(\Psi_A - \Psi_C)]c_{r,b}} \\ & \times \left\{\frac{V}{k}\left(1 + \ln\left(\frac{\alpha_f L_0}{V}\right) - \frac{\alpha_f L_0}{V}e^{-kl}\right)\left[1 - \frac{c_r}{C\omega(\Psi_A - \Psi_C)}\right] - lc_l - c_f F - \frac{\alpha_s(\gamma + 1)}{\alpha_w}G_u\right\}\end{aligned} \tag{A49}$$

when $l > l^{\sim}$. Thus, the time it takes for leaves to grow from l_u to $l^{\sim}$ is

$$t_y = \frac{c_{l,b} + [V/C\omega(\Psi_A - \Psi_C)]c_{r,b}}{V - c_l - [V/C\omega(\Psi_A - \Psi_C)]c_r}\ln\left(\frac{l^{\sim}\{V - c_l - [V/C\omega(\Psi_A - \Psi_C)]c_r\} - [\alpha_s(\gamma + 1)/\alpha_w]G_u}{l_u\{V - c_l - [V/C\omega(\Psi_A - \Psi_C)]c_r\} - [\alpha_s(\gamma + 1)/\alpha_w]G_u}\right), \tag{A50}$$

and the time it takes for leaves to grow from $l^{\sim}$ to l_c is t_z. We found no closed-form solution for t_z. For our purposes, we estimated t_z by using a simple numerical approximation. To be conservative in the approximation, we used the beginning of the interval to project leaves forward. We made sure that the estimate of t_z saturated to 1% accuracy. The total time of the transition, then, is $t_L = t_x + t_y + t_z$.

If we take the yearly average soil-water potential, $\Psi_A = -0.75$, use the parameter values listed in table A1, and

numerically estimate t_z, we find t_L is just 20% of the growing season of one year (about 7 weeks). This is a very small amount of time, compared to the total expectation of time a tree would live in the canopy, 63 growing seasons ($\mu_c = 0.016$).

To see just how big this effect is, we look at the expected fecundity of a tree, given that it has reached the understory. The t_L affects both D^* and LRS, but because it will only make D^* smaller and give trees larger lifetime fecundity, the opposite of our concern for the effect on LRS, we consider D^* independent of t_L here, and the expected fecundity of a tree, given that it has reached the canopy, is

$$\mathrm{LRS}_{\text{canopy tree}} = F_c \frac{G_c^{\gamma}}{\mu_c^{\gamma+1}} \Gamma(\gamma + 1) e^{(\mu_c/G_c)(D^* + G_u t_L) + \mu_c t_L}. \tag{A51}$$

Figure A4 shows the dependence of a canopy tree's expected output in terms of fecundity. In the main text, we approximate this as $t_L = 0$. Here, we have estimated that t_L is actually 0.2, the first line drawn in figure A4. For perspective, a second line, for t_L of 4 years, is drawn.

It is therefore reasonable for our scale of predictions to use the approximation that trees immediately switch leaf and root investments and obtain canopy growth rates at the moment they grow out of the understory,

$$\mathrm{LRS} \approx e^{-(\mu_u/G_u)D^*} \int_0^{\infty} e^{-\mu_c \tau} F_c \alpha_w (D^* + G_c \tau)^{\gamma} d\tau. \tag{A52}$$

With constant vital rates in the understory and the canopy, we are able to use the methods for determining population dynamics and stability of species in the perfect-plasticity approximation (Strigul et al. 2008).

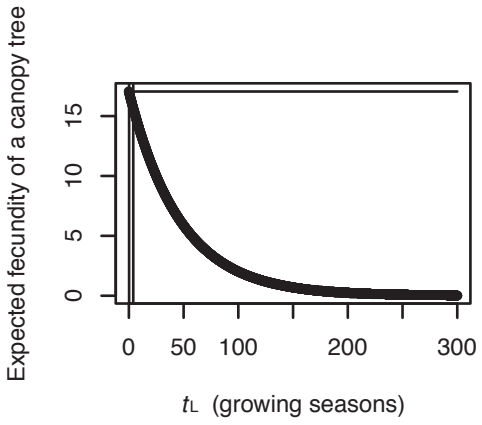

Figure A4: Dependence of a canopy tree's expected fecundity on the time it takes to transition to canopy leaf and root traits, t_L. This is an example with the parameter values described in the text included. Our approximation of a canopy tree's fecundity ($t_L = 0$) is represented by the horizontal line. The estimated likely t_L (0.2 growing seasons) is shown as the first vertical line. The second vertical line represents a realistic maximal value of t_L, 4 years. From this plot, we can see that our approximation is reasonable for the types of forests we discuss in the article.

Stability of the Dynamic Equilibrium

For a closed-canopy forest in our model, the equilibrial size distribution can be shown to be locally stable. If a few trees are killed or a few trees are planted, the forest will return over time to the same size distribution, with the same equilibrium height of canopy closure (Z^*) and resource availability.

Immediately after a perturbation (cutting or adding a few trees), Z^* will be perturbed a bit and some trees will be promoted into the canopy earlier than expected or put back in the shade. As we saw in "Timescale of Transition to Canopy Leaf Area Index and Root Area Index," after a plant has moved from the understory into the canopy, it is able to increase its leaf area index and fine-root area index to its canopy strategy rapidly. A plant that is moved from the canopy

to the understory should be able to decrease the leaves and fine roots it holds even faster. After this shift happens, the light level in the understory will return to its value before the perturbation. The water uptake of the canopy plants returns to the original level, and the understory still accounts for a negligible portion of this uptake. After the rapid adjustment of leaves and fine roots following the disturbance, then, the canopy and understory growth rates will return to their predisturbance values. A perturbed tree size distribution and Z^* are now the only signs of disturbance. Stability in the face of these perturbations is proven by Strigul et al. (2008).

It is important to note that the closed-canopy criterion, equation (A20), may be satisfied even if the equilibrium Z^* is not stable. Such species cast such deep shade that their understory trees are unable to maintain a positive carbon balance to grow. Unstable cases produce stands in which trees grow up from a major disturbance together, and only after enough of those trees have died to open the ground area will new trees begin to grow again. These forests will have fluctuating resource levels and values of D^* unlike those in the cases we analyze. Results of this article focus on conditions that satisfy equation (A20) and have a $G_u > 0$ and thus have satisfied stability criteria.

Z^* Derivation

Strigul et al. (2008) provide a full derivation of the height of canopy closure Z^* for a monoculture of trees with a crown area–to-diameter allometric exponent γ of 2. Here, we derive the result for arbitrary values of γ.

We begin with equation (1) of Strigul et al. (2008), which defines Z^* as the height at which the sum of all pieces of crown taller than it equal the ground area,

$$1 = \int_{Z^*}^{\infty} N(Z)A(Z^*, Z)dZ, \tag{A53}$$

where $N(Z)$ is the density of trees of height Z and $A(Z^*, Z)$ is the crown area of the portion of a tree of height Z that is above Z^*. For flat-top trees, this is equal to the whole crown area of trees taller than Z^*,

$$1 = \int_{Z^*}^{\infty} N(Z)W(Z)dZ. \tag{A54}$$

Using the allometries of equation (A1) and switching to a diameter size index,

$$1 = \int_{D^*}^{\infty} N(D)\alpha_w D^{\gamma}dD, \tag{A55}$$

where D^* is $(Z^*/H)^{1/(\gamma-1)}$, or the diameter at which trees transition from the understory to the canopy. Equation (25) of Strigul et al. (2008) gives the equilibrial density of trees of diameter D for $D > D^*$,

$$\hat{N}(D) = \frac{F}{G_c} e^{-(\mu_u/G_u)D^*} e^{-(\mu_c/G_c)(D-D^*)}, \tag{A56}$$

which is just the amount of total fecundity per unit area per year, F, left over after spending D^*/G_u dying at a rate μ_u and $(D - D^*)/G_c$ dying at a rate μ_c. This result is derived in Strigul et al. (2008) from the von Foerster equations for a model of continuous population growth.

Equation (A55) can be rearranged to

$$1 = \frac{F\alpha_w G_c^{\gamma}}{\mu_c^{\gamma+1}} e^{-[(\mu_u/G_u)-(\mu_c/G_c)]} \int_{(\mu_c/G_c)D^*}^{\infty} e^{-x}x^{\gamma}dx. \tag{A57}$$

Table A2 provides references for the following parameter values: $\mu_c \approx 0.016$ year^{-1}, $G_c \approx 0.6$ cm year^{-1}, and $D^* \approx 2.36$

cm (for $Z^* = 20$ m). This makes the limits of integration 0.06 and infinity. Because 0.06 is much less than the peak of the integrand (γ, 1.5), integrating the function from 0 to infinity instead of from 0.06 to infinity introduces an error of only 0.05%. With this approximation, we find that the diameter of the smallest trees in the canopy can be expressed explicitly in terms of vital rates of the species:

$$D^* \approx \frac{1}{(\mu_u/G_u) - (\mu_c/G_c)} \ln\left(\frac{F\alpha_w G_c^\gamma \Gamma(\gamma + 1)}{\mu_c^{\gamma+1}}\right). \tag{A58}$$

For simplicity in this article, we use an additional approximation valid when $\mu_c/G_c \ll \mu_u/G_u$. This step is not necessary for the tractability of successive derivations, but it makes our analyses more easily accessible to the reader without losing biological insight:

$$D^* \approx \frac{G_u}{\mu_u} \ln\left(\frac{F\alpha_w G_c^\gamma \Gamma(\gamma + 1)}{\mu_c^{\gamma+1}}\right). \tag{A59}$$

Table A2. Detailed sources of parameter estimates

Variable	Description	Units	Estimate	Source
Tree measurements:				
μ	Mortality rate	$year^{-1}$	$\mu_c = .016$; $\mu_u = .038$	Purves et al. 2008; "Individual Trees" in appendix A; species average, mesic soil
F	Fecundity	saplings m^{-2} $year^{-1}$	$F_c = .0071$;	Purves et al. 2008; "Individual Trees" in appendix A
H	Allometric constant ($Z = HD^{\gamma-1}$)	$m/cm^{\gamma-1}$	3.6	Calculated from data of the Forest Health Monitoring program of the Forest Service (Woodall et al. 2010)
α_w	Allometric constant ($W = \alpha_w D^{\gamma}$)	m^2/cm^{γ}	.20	Calculated from data of the Forest Health Monitoring program of the Forest Service (Woodall et al. 2010)
α_s	Allometric constant ($S = \alpha_s D^{\gamma+1}$)	kg $C/cm^{\gamma+1}$	.0815	Dybzinski et al. 2011 analysis of Jenkins et al. 2003 and White et al. 2000 data
γ	Allometric exponent		1.5	See "Tree Structure"
Carbon assimilation and allocation:				
c_l	Cost of building and maintaining leaf biomass, including sapwood respiration	kg C m^{-2} $year^{-1}$	.187	Foliage and sapwood respiration per square meter. Foliage building cost was taken by averaging leaf mass per unit area values for sun and shade leaves and adding a 20% building respiration cost. Respiration rates also came from averaging sun and shade leaves of deciduous trees (Chen et al., forthcoming). Sapwood respiration is calculated from Bolstad et al.'s 2004 measured value of yearly 2.33 Mg C ha^{-1} $year^{-1}$ divided by a leaf area index of 5 (their table 4).
c_r	Cost of building and maintaining roots	kg C m^{-2} $year^{-1}$	.044	Fine-root respiration. Building and maintenance respiration of roots is 1.25 kg C kg C^{-1} (Shevliakova et al. 2009). We assumed a fine-root life span of 2 years. Surface area of fine roots per kilogram carbon, 44.6 m^2, was calculated from Jackson et al. 1997.
c_f	Cost of fecundity	kg C $sapling^{-1}$	4.87	Dybzinski et al. 2011 analysis of Whittaker et al. 1974
Water-saturated photosynthesis:				
V	Maximal rate of carbon fixation	kg C m^{-2} $year^{-1}$	.6	Known to be variable across environmental conditions, across species, and within species. Yearly estimates are difficult to calculate. Here we use a V that gives a reasonable number for the gross primary productivity of a water-saturated temperate forest, about 2.5 kg C m^{-2} $year^{-1}$.
α_f	Relationship between carbon fixation and light intensity	kg C $(MJ\ PAR)^{-1}$	.001	As with V, yearly estimates are difficult to calculate directly. We use an α_f that allows the first two leaf layers in the canopy to operate at V.
Water-limited photosynthesis:				
C	Water conductance from soil to fine roots	m MPa^{-1} m^{-2} $year^{-1}$	.29	Maximum transpiration (Rodríguez-Iturbe and Porporato 2004, p. 299)/typical root area index (Jackson et al. 1997)/(saturating soil-water potential − wilting water potential (Rodríguez-Iturbe and Porporato 2004, p. 299))
ω	Water-use efficiency	kg C m^{-1}	2	Eamus et al. 2006 (p. 14) reports .79 tons C $year^{-1}$ km^{-2} mm^{-1} rain, and Larcher 2003 (p. 295) reports that 67% of precipitation in deciduous forests is transpired
Ψ_C	Critical xylem water potential	MPa	−2.5	Rodríguez-Iturbe and Porporato 2004, p. 299

Note: PAR = photosynthetically active radiation.

Literature Cited Only in the Appendix

Adams, T. P., D. W. Purves, and S. W. Pacala. 2007. Understanding height-structured competition in forests: is there an *R** for light? Proceedings of the Royal Society B: Biological Sciences 274:3039–3047.

Bolstad, P. V., K. J. Davis, J. Martin, B. D. Cook, and W. Wang. 2004. Component and whole-system respiration fluxes in northern deciduous forests. Tree Physiology 24:493–504.

Chen, A., J. W. Lichstein, J. L. D. Osnas, and S. W. Pacala. Forthcoming. Species-independent down-regulation of leaf photosynthesis and respiration in response to shading: evidence from six temperate forest tree species. Canadian Journal of Forest Research.

Eamus, D., T. Hatton, P. Cook, and C. Colvin. 2006. Ecohydrology: vegetation function, water and resource management. CSIRO, Collingwood, Australia.

Jackson, R. B., H. A. Mooney, and E.-D. Schulze. 1997. A global budget for fine root biomass, surface area, and nutrient contents. Proceedings of the National Academy of Sciences of the USA 94:7362–7366.

Jenkins, J. C., D. C. Chojnacky, L. S. Heath, and R. A. Birdsey. 2003. National-scale biomass estimators for United States tree species. Forest Science 49:12–35.

Kumagai, T., H. Nagasawa, T. Mabuchi, S. Ohsaki, K. Kubota, K. Kogi, Y. Utsumi, S. Koga, and K. Otsuki. 2005. Sources of error in estimating stand transpiration using allometric relationships between stem diameter and sapwood area for *Cryptomeria japonica* and *Chamaecyparis obtusa*. Forest Ecology and Management 206:191–195.

Lambert, M.-C., C.-H. Ung, and F. Raulier. 2005. Canadian national tree aboveground biomass equations. Canadian Journal of Forest Research 35:1996–2018.

Larcher, W. 2003. Physiological plant ecology: ecophysiology and stress physiology of functional groups. Springer, New York.

Lichstein, J. W., J. Dushoff, K. Ogle, A. Chen, D. W. Purves, J. P. Caspersen, and S. W. Pacala. 2010. Unlocking the forest inventory data: relating individual tree performance to unmeasured environmental factors. Ecological Applications 20:684–699.

Longuetaud, F., F. Mothe, J. M. Leban, and A. Makela. 2006. *Picea abies* sapwood width: variations within and between trees. Scandinavian Journal of Forest Research 21:41–53.

McMahon, T. 1973. Size and shape in biology: elastic criteria impose limits on biological proportions, and consequently on metabolic rates. Science 179:1201–1204.

Paw, U. K. T., and W. Gao. 1988. Applications of solutions to non-linear energy budget equations. Agricultural and Forest Meteorology 43:121–145.

Rodríguez-Iturbe, I., and A. Porporato. 2004. Ecohydrology of water-controlled ecosystems: soil moisture and plant dynamics. Cambridge University Press, Cambridge.

Shevliakova, E., S. W. Pacala, S. Malyshev, G. C. Hurtt, P. C. D. Milly, J. P. Caspersen, L. T. Sentman, J. P. Fisk, C. Wirth, and C. Crevoisier. 2009. Carbon cycling under 300 years of land use change: importance of the secondary vegetation sink. Global Biogeochemical Cycles 23:GB2022.

White, M. A., P. E. Thornton, S. W. Running, and R. R. Nemani. 2000. Parameterization and sensitivity analysis of the BIOME-BGC terrestrial ecosystem model: net primary production controls. Earth Interactions 4(3):1–85.

Whittaker, R. H., F. H. Bormann, G. E. Likens, and T. G. Siccama. 1974. The Hubbard Brook Ecosystem Study: forest biomass and production. Ecological Monographs 44:233–252.

Woodall, C. W., B. L. Conkling, M. C. Amacher, J. W. Coulston, S. Jovan, C. H. Perry, B. Shulz, G. C. Smith, and S. Will-Wolf. 2010. The Forest Inventory and Analysis Database version 4.0: database description and users manual for phase 3. General Technical Report NRS-61. U.S. Forest Service, Newtown Square, PA.

Appendix B from C. Farrior et al., "Competition for water and light in closed-canopy forests: a tractable model of carbon allocation with implications for carbon sinks" *The American Naturalist*.

UNDERSTORY RESULTS

The understory ESS strategies are dependent on the canopy strategies, which alter the light level available to understory trees ($L_\mathrm{U} = L_0\, e^{-k\ x\ l_\mathrm{c}}$) and the water availability of the stand ($\Psi_\mathrm{A}\ \frac{R}{r\ C} + \Psi_\mathrm{C}$). Analytical results for understory ESS strategies and their illustration are presented in Table B1 and illustrated in Figure B1.

If the canopy is water saturated (Case 1), the understory, which has less light than the canopy, is also water-saturated. Understory ESS strategies follow similar formulae for their ESS investment strategies, where only the light level at the top of the canopy differs. In Case 4, when the canopy is co-limited on wet days and water-limited on dry days, an understory plant with ESS leaf and fine-root allocation is co-limited throughout the whole season. Here understory plants have only the leaves they can utilize and only enough fine-roots to support their leaves.

Both Case 2 and 3 are the same for the understory perspective. The understory is co-limited on dry days and water saturated on wet days. The ESS leaf allocation strategy is equivalent to the canopy strategy under similar limitation conditions, with only the difference in light availability. The fine-root strategy of these plants differs significantly from canopy plants, however. Because the understory has far less water uptake than the canopy trees, the understory strategy in fine-root investment is not influenced by competition with other understory individuals. Because the competitive canopy individuals have created an environment where each additional bit of fine-root biomass provides no benefits during water-limitation, there exists a set of strategies for the understory that are equivalent, making the reported $r_\mathrm{u}^\mathrm{ESS}$ in the table not a true ESS in this model (range of these strategies is presented in Table B1).

This neutrality among strategies within the listed range depends on the assumption that the canopy plants have fine-root surface area per unit area exactly equal to the ESS. This seems unlikely given the ubiquity of small disturbances and variation in environment from year to year. For the moment, we will call the fine-root surface area per unit area realized by the canopy plants, $r_\mathrm{c}^\mathrm{ENV}$. If $r_\mathrm{c}^\mathrm{ENV} > r_\mathrm{c}^\mathrm{ESS}$, $r_\mathrm{u}^\mathrm{ESS}$ is a single convergence stable ESS that equals the upper bound of the neutral range (* in Table B1). If $r_\mathrm{c}^\mathrm{ENV} < r_\mathrm{c}^\mathrm{ESS}$, $r_\mathrm{u}^\mathrm{ESS}$ is a single convergence stable ESS that equals the lower bound of the neutral range.

Table B1: Understory ESS allocation patterns.

Canopy Case	$l_\mathrm{u}^\mathrm{ESS}$	$r_\mathrm{u}^\mathrm{ESS}$
1	$\frac{1}{k}\ln\left(\frac{\alpha_\mathrm{f}\ L_\mathrm{U}}{c_\mathrm{l}}\right)$	$\frac{A_\mathrm{L}(L_\mathrm{U}, l_\mathrm{u}^\mathrm{ESS})}{C\ \omega\ (\Psi_\mathrm{B} - \Psi_\mathrm{C})}$
2 & 3	$\frac{1}{k}\ln\left(\frac{q\ \alpha_\mathrm{f}\ L_\mathrm{U}}{c_\mathrm{l}}\right)$	within*: $(\frac{A_\mathrm{L}(L_\mathrm{U}, l_\mathrm{u}^\mathrm{ESS})}{C\ \omega\ (\Psi_\mathrm{B} - \Psi_\mathrm{C})}, \frac{A_\mathrm{L}(L_\mathrm{U}, l_\mathrm{u}^\mathrm{ESS})}{C\ \omega\ (\Psi_\mathrm{A} - \Psi_\mathrm{C})})$
4	$\frac{1}{k}\ln\left(\frac{q\ \alpha_\mathrm{f}\ L_\mathrm{U}}{c_\mathrm{l}}\right)$	$\frac{A_\mathrm{L}(L_\mathrm{U}, l_\mathrm{u}^\mathrm{ESS})}{C\ \omega\ (\Psi_\mathrm{B} - \Psi_\mathrm{C})}$

Analytical expressions of ESS understory leaf and fine-root area per unit individual crown area. L_U and Ψ_A depend on canopy strategies of the canopy plants that differ among cases. $*$Range of fine-root strategies competitively dominant to other potential strategies. See text of this appendix for further explanation.

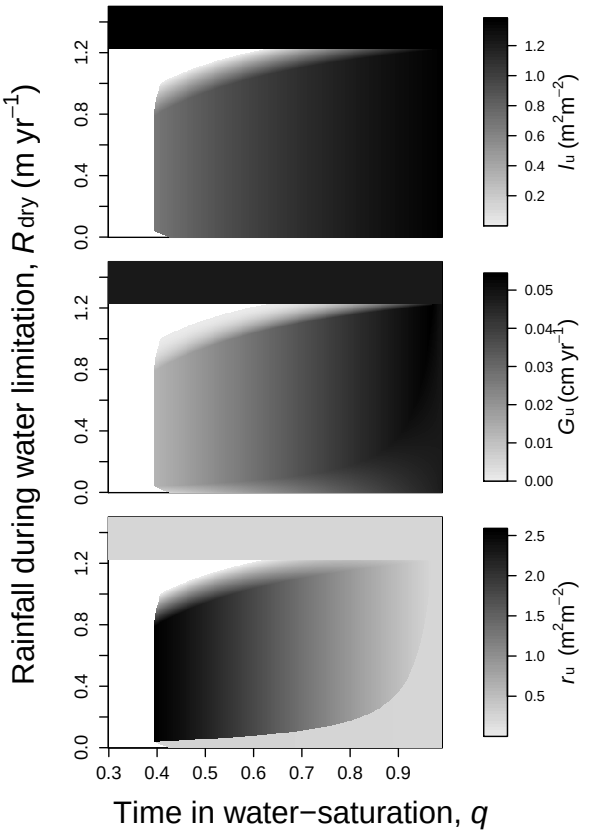

Figure B1: Understory leaf, woody biomass and fine-root investment of the competitive-dominant species along two axes of rainfall variability, the portion of the growing season in water saturation (q) and the rainfall rate during the water-limited portion (R_{dry}). Conditions become wetter as you move from up and to the right in each panel. Analytical results for each point can be found in Table B1.

Appendix C from C. Farrior et al., "Competition for water and light in closed-canopy forests: a tractable model of carbon allocation with implications for carbon sinks" *The American Naturalist*.

PAIRWISE INVASION PLOTS

To determine the plant allocation ESSs presented in Table 2 of the printed paper analytical methods were used. To check that these ESSs are global and convergence stable we numerically verified several cases. Here we present one such verification for each of the analytical cases (1-4). These verifications are presented as pairwise invasion plots where the following conditions are represented by the following colors:

Green	$\mathrm{LRS}(G,B) > 1$	$\mathrm{LRS}(B,G) < 1$
Blue	$\mathrm{LRS}(G,B) < 1$	$\mathrm{LRS}(B,G) > 1$
Yellow	$\mathrm{LRS}(G,B) > 1$	$\mathrm{LRS}(B,G) > 1$
Gray	$\mathrm{LRS}(G,B) = 1$	$\mathrm{LRS}(B,G) = 1$
Purple	$\mathrm{LRS}(G,B) < 1$	$\mathrm{LRS}(B,G) < 1$

where G is the "Green Strategy" and B is the "Blue Strategy". Black boxes mark the analytically derived and numerically evaluated for each case. The range of trait values presented in each case is the range of traits that produce a closed-canopy forest in monoculture under the given conditions. The white line in each plot indicates the 1:1 line.

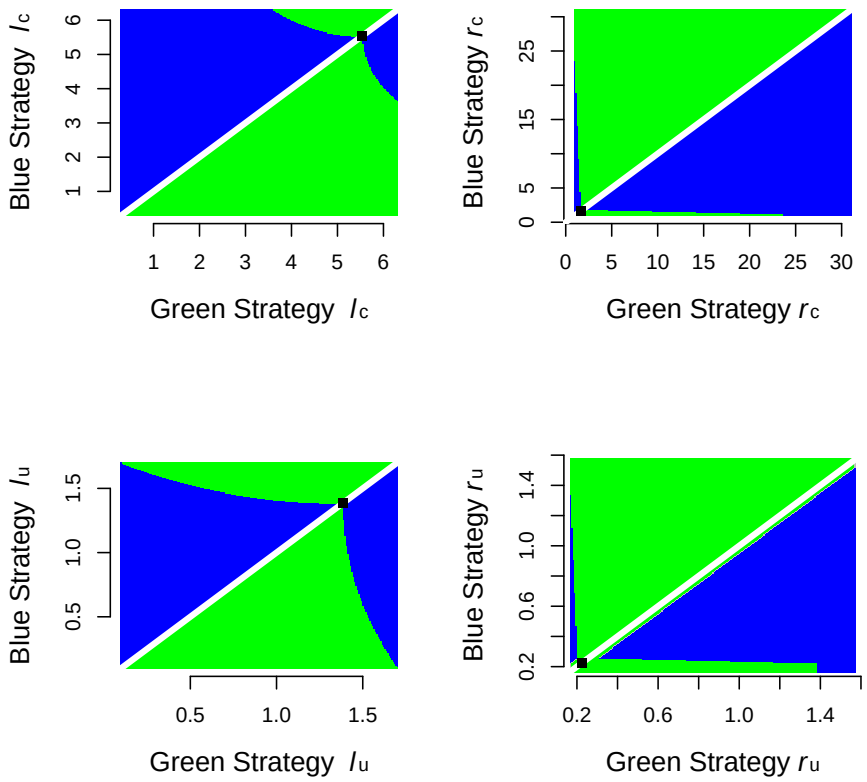

Figure C1: Case 1 pairwise invasion plot. $R_{\text{wet}} = 1.5\,\text{m}/\text{m}^2/\text{yr}$, $R_{\text{dry}} = 1.45\,\text{m}/\text{m}^2/\text{yr}$ and $q = 0.2$.

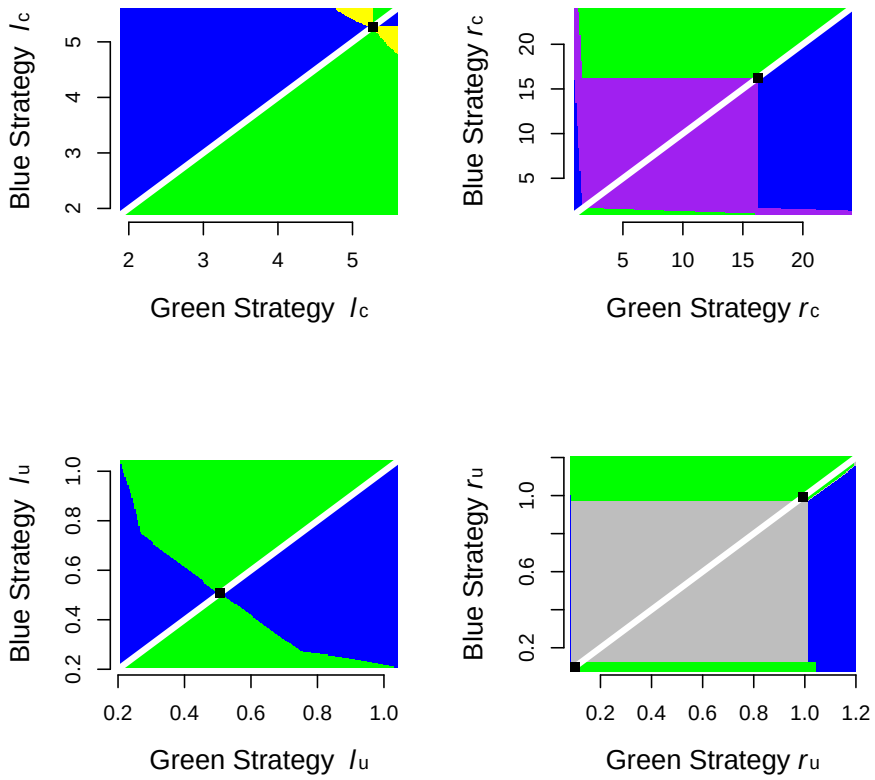

Figure C2: Case 2 pairwise invasion plot. $R_{\text{wet}} = 1.5\ \text{m}/\text{m}^2/\text{yr}$,$R_{\text{dry}} = 1.2\ \text{m}/\text{m}^2/\text{yr}$ and $q = 0.7$. If fine-root surface area per unit area in the environment ($r_{\text{c}}^{\text{ENV}}$) is exactly equal to $r_{\text{c}}^{\text{ESS}}$, there is no single ESS for the understory fine-root strategy, r_u. In the r_{u} panel, black boxes indicate the range of strategies competitively dominant to those outside the range. If $r_{\text{c}}^{\text{ENV}} < r_{\text{c}}^{\text{ESS}}$, $r_{\text{u}}^{\text{ESS}}$ is a single convergence stable ESS equal to the value of the upper black box. If $r_{\text{c}}^{\text{ENV}} > r_{\text{c}}^{\text{ESS}}$, $r_{\text{u}}^{\text{ESS}}$ is a single convergence stable ESS equal to the value of the lower black box (see Appendix B for further explanation).

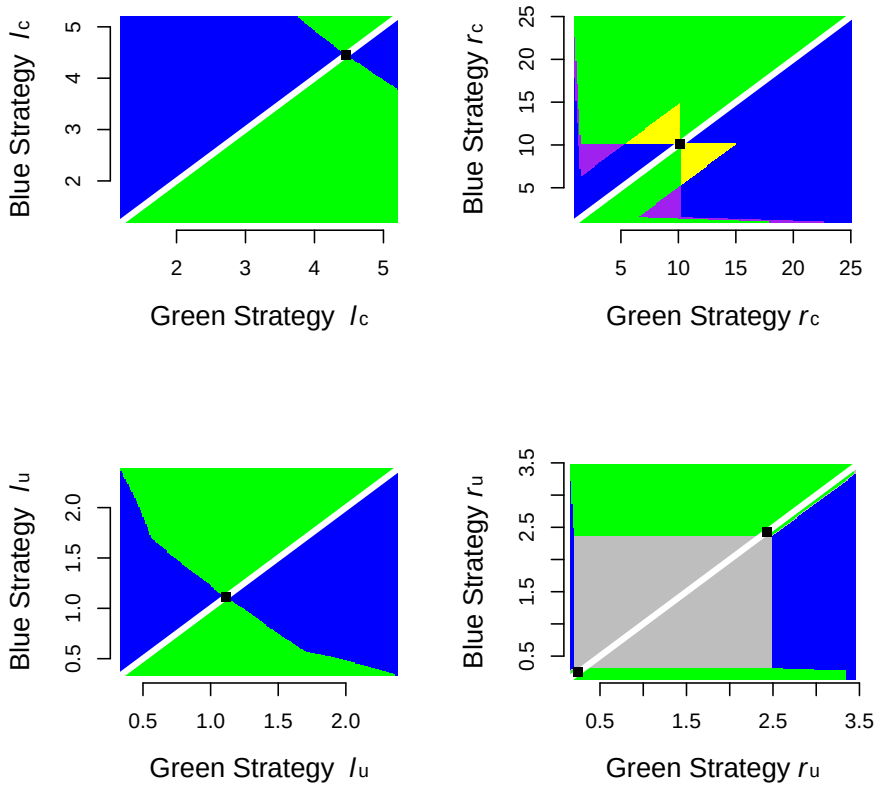

Figure C3: Case 3 pairwise invasion plot. $R_{\text{wet}} = 1.5\ \text{m}/\text{m}^2/\text{yr}$, $R_{\text{dry}} = 0.75\ \text{m}/\text{m}^2/\text{yr}$ and $q = 0.7$. If fine-root surface area per unit area in the environment ($r_{\text{c}}^{\text{ENV}}$) is exactly equal to $r_{\text{c}}^{\text{ESS}}$, there is no single ESS for the understory fine-root strategy, r_u. In the r_{u} panel, black boxes indicate the range of strategies competitively dominant to those outside the range. If $r_{\text{c}}^{\text{ENV}} < r_{\text{c}}^{\text{ESS}}$, $r_{\text{u}}^{\text{ESS}}$ is a single convergence stable ESS equal to the value of the upper black box. If $r_{\text{c}}^{\text{ENV}} > r_{\text{c}}^{\text{ESS}}$, $r_{\text{u}}^{\text{ESS}}$ is a single convergence stable ESS equal to the value of the lower black box (see Appendix B for further explanation).

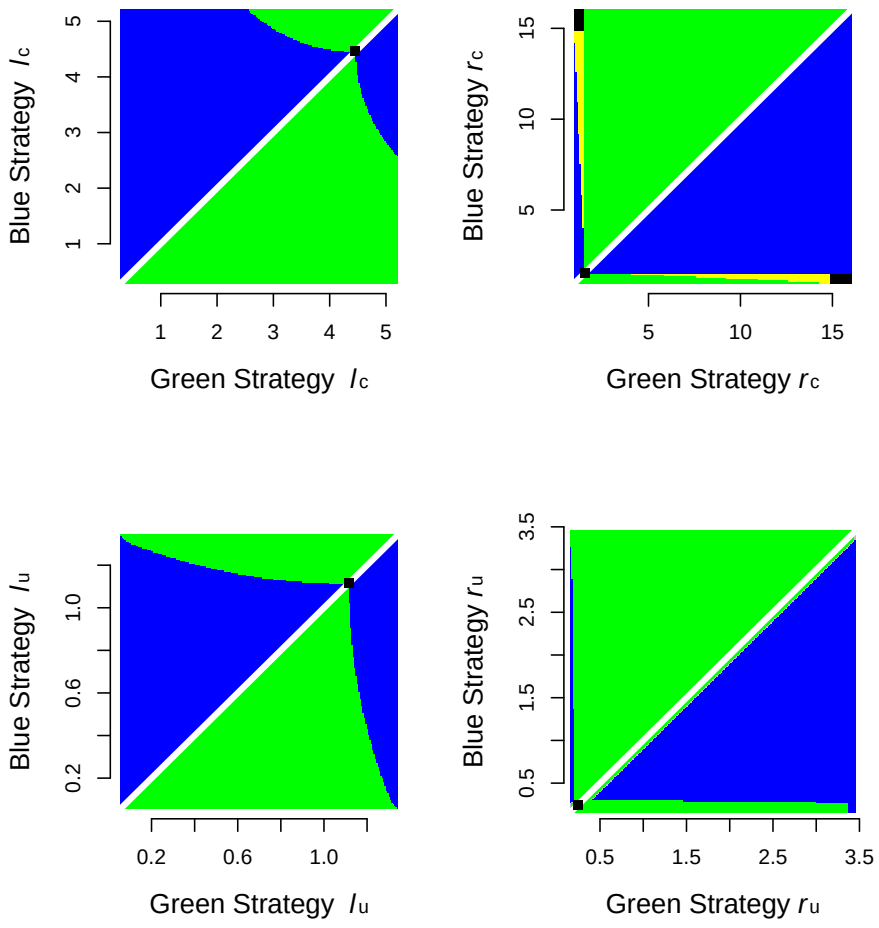

Figure C4: Case 4 pairwise invasion plot. $R_{\text{wet}} = 1.5\ \text{m}/\text{m}^2/\text{yr}$, $R_{\text{dry}} = 0.1\ \text{m}/\text{m}^2/\text{yr}$ and $q = 0.7$.